

# 行政院國家科學委員會專題研究計畫 成果報告

## 費米能階釘扎效應, 準分子雷射加工與乾蝕刻技術應用於 P 型氮化鎵蕭特基二極體製作之研究

計畫類別：個別型計畫

計畫編號：NSC93-2215-E-018-005-

執行期間：93 年 08 月 01 日至 94 年 07 月 31 日

執行單位：國立彰化師範大學光電工程技術研究所

計畫主持人：林祐仲

計畫參與人員：朱宥霖, 林文祥, 吳國禎

報告類型：精簡報告

處理方式：本計畫可公開查詢

中 華 民 國 94 年 7 月 4 日

#### **研究計畫中文摘要：**

關鍵字： 氮化鎵，蕭特基二極體，表面費米能階釘扎，乾蝕刻

目前，氮化鎵族群的藍色發光二極體及雷射的性能提昇上，除必須有良好的磊晶結構之外，必須有性能良好的 p 型及 n 型歐姆接觸特性。由於目前 p 型氮化鎵磊晶層之電洞濃度無法有效的提高，因此要達到金屬/p 型氮化鎵的歐姆接觸較為困難。在 p 型氮化鎵的歐姆接觸研究已有諸多成果被發表，反觀 p 型氮化鎵的蕭特基接觸的研究並不多，其已發表之文獻報導所觀測的位障高度差異甚大，並未有明確的機制被建立。此次研究將主持人先前對 p 型氮化鎵的歐姆接觸的研究成果應用於 p 型氮化鎵蕭特基二極體中歐姆電極製作，因為良好歐姆電極將有助提昇 p 型氮化鎵蕭特基二極體之電特性，此外，再利用乾蝕刻處理(反應離子蝕刻或感應耦合電漿蝕刻技術)或準分子雷射加工處理產生 p 型氮化鎵表面施體型缺陷引發費米能階釘扎效應提高 p 型氮化鎵蕭特基二極體之蕭特基電極與 p 型氮化鎵間之障壁，降低漏電流。本次計畫成果將有助於對 p 型氮化鎵之材料特性有所了解、製作優良之 p 型氮化鎵蕭特基二極體，而且也能改善金屬/p 型氮化鎵的歐姆接觸進而提高藍光二極體的效能。另一方面，對於發展氮化鎵的光檢測也有極大的助益。

#### **研究計畫英文摘要：**

Keywords: GaN, Schottky diodes, Barrier height, Surface Fermi level pinning,

Dry etching

GaN continues to grow in importance for the high-brightness light emitting diodes (LEDs) in the visible and ultraviolet wavelength regions. For the case of the highly efficient LED, several critical problems must be addressed, such as high hole concentration in p-type GaN (p-GaN) and low-resistance ohmic contact in the fabrication processes for the devices. High-quality ohmic and Schottky contacts are required for the improvement of these devices. The ohmic-contact characteristics of metal contact on p-GaN have been relatively established. Only a few studies of barrier height on p-GaN have been reported in the literature, likely due to the difficulties in measuring diodes with large leakage and large series resistance. The contacts tend to exhibit very leaky Schottky characteristics. Consequently, the mechanism of current flow through the interface has not been established and the exact value of Schottky barrier height has not yet been estimated. The p-GaN ohmic-contact technique reported in our previous published paper shall be applied in this study. Good ohmic contacts will help to obtain the actual p-GaN Schottky characteristics. In addition, the applications of the dry etching and an excimer laser treatment in the fabrication of p-GaN Schottky contacts will induce the formation of the surface defects on the p-GaN surface, the pinning of the Fermi level on the p-GaN surface and the enhancement of the Schottky barrier height at the metal/p-GaN interface. So in this plan, we are devoted to improve the p-GaN Schottky contact.

#### 計畫成果自評：

本次計畫研究內容與原計畫相符程度達 80%，並達成預期目標，而且研究成果五篇論文均已發表於國際知名期刊，獲得國際學者肯定，極具學術與實際應用之價值。

#### 結案報告內容：

此次專題計畫研究成果已撰寫成五篇論文並發表於美國國際期刊，依序列於下：

1. **Y. J. Lin**, 2005, March “Application of the thermionic field emission model in the study of a Schottky barrier of Ni on p-GaN from current-voltage measurements”, Appl. Phys. Lett. Vol.86, 122109.
2. **Y. J. Lin** and Y. L. Chu, 2005, May “Effect of reactive ion etching-induced defects on the surface band bending of heavily Mg-doped p-type GaN”, J. Appl. Phys. Vol.97, 104904.
3. **Y. J. Lin**, Y. L. Chu, Y. S. Huang, and H. C. Chang, 2005, May “Optical and electrical properties of heavily Mg-doped GaN upon  $(\text{NH}_4)_2\text{S}_x$  treatment”, Appl. Phys. Lett. Vol.86, 202107.
4. **Y. J. Lin**, 2005, Jan./Feb. “Electrical properties of Ni/Au and Au contacts on p-type GaN”, J. Vac. Sci. Technol. B Vol.23, 48.
5. **Y. J. Lin** and C. W. Hsu, 2004, Sep. “Study of Schottky barrier heights of indium-tin-oxide on p-GaN using x-ray photoelectron spectroscopy and current-voltage measurements”, J. Electron. Mater. Vol.33, 1036.

論文詳細內容如下所示：

# Application of the thermionic field emission model in the study of a Schottky barrier of Ni on *p*-GaN from current–voltage measurements

Yow-Jon Lin<sup>a)</sup>

Institute of Photonics, National Changhua University of Education, Changhua 500, Taiwan, Republic of China

(Received 24 May 2004; accepted 7 February 2005; published online 18 March 2005)

Barrier height values of Ni contacts to Mg-doped *p*-type GaN (*p*-GaN) were obtained from current–voltage measurements in this study. The induced deep level defect band through high Mg doping led to a reduction of the depletion layer width in the *p*-GaN near the interface and an increase in the probability of thermionic field emission. It also resulted in an increase in current flow under forward bias condition, which was not analyzed using the thermionic emission model. Further, the calculated barrier height value of Ni contacts to *p*-GaN using the thermionic field emission model is in good agreement with the value of 1.9 eV obtained from x-ray photoelectron spectroscopy measurements. © 2005 American Institute of Physics. [DOI: 10.1063/1.1890476]

GaN has a 3.4 eV direct gap at room temperature and has attracted a lot of interest because of its application to optical devices in the short-wavelength region. Other devices that have been demonstrated so far include ultraviolet Schottky barrier photodetectors, solar-blind Schottky photodiodes, metal–semiconductor field effect transistors, and high electron mobility transistors.<sup>1–4</sup> High-quality ohmic and Schottky contacts are required for the improvement of these devices. Since the sum of the barrier height of the *n* and *p* types equals the band gap 3.4 eV, a high barrier height is expected after the metals have been deposited on the *p*-GaN.<sup>5</sup> Recent reviews and studies of Schottky contact properties on *p*-GaN have been published.<sup>6–11</sup> Some reported values for barrier height for different metals are 0.49–0.50 eV for Pt,<sup>6,8</sup> 0.57 eV for Au,<sup>6</sup> 0.65 eV for Ti,<sup>6</sup> and 1.3 eV for Pd.<sup>9</sup> For Ni there is a fairly large discrepancy in reported values, ranging from 0.49 to 2.87 eV.<sup>6,7,10,11</sup> Consequently, the mechanism of current flow through the interface has not been established and the exact value of the barrier height has not yet been estimated using the current–voltage (*I*–*V*) measurement. The observed barrier height value from capacitance–voltage (*C*–*V*) measurements has been reported.<sup>7</sup> However, Yu *et al.*<sup>7</sup> did not obtain the barrier height value from the *I*–*V* measurements. In this study, the barrier height value of the Ni/*p*-GaN samples was first successfully obtained from the *I*–*V* measurements. Further, the calculated barrier height value of Ni contacts to *p*-GaN using the thermionic field emission (TFE) model is in good agreement with the value of 1.9 eV obtained from x-ray photoelectron spectroscopy (XPS) measurements.

The epitaxial layers used in the experiments were grown on *c*-plane sapphire substrates using a metalorganic chemical vapor deposition system. Trimethylgallium, ammonia, and bis-cyclopentadienylmagnesium were used as the Ga, N, and Mg sources, respectively. An undoped GaN buffer layer with a thickness of 650 nm was grown on the sapphire substrate at 520 °C, followed by the growth of a Mg-doped *p*-GaN layer (762 nm) at 1100 °C. Mg concentration ( $[Mg]$ ) was  $\sim 6 \times 10^{19} \text{ cm}^{-3}$  for all samples. The grown samples were annealed for the purpose of generating holes at 750 °C for

30 min in N<sub>2</sub> ambient. According to the Van der Pauw–Hall measurements, we calculated the hole concentration to be  $3.6 \times 10^{17} \text{ cm}^{-3}$ . The samples were cleaned in chemical clean solutions of trichloroethylene, acetone, and methanol. Planar-type Schottky contacts were formed by electron-beam evaporation. Using the lift-off technique, Ni/Au (5 nm/5 nm) ohmic contacts were deposited and annealed at 500 °C in air ambient for 10 min. The fabricated process of ohmic contacts combined with the low specific contact resistance has been previously reported.<sup>12</sup> Good ohmic contacts help to obtain the actual Schottky characteristics from *I*–*V* measurements. Then, Ni (5 nm) Schottky contact with circular patterns (200  $\mu\text{m}$  in diameter) was directly deposited. The Schottky diodes were measured by the *I*–*V* method using a Keithley Model-4200-SCS/F semiconductor characterization system at 300, 350 and 400 K, respectively.

Figure 1 shows the typical semilog current density–voltage (*J*–*V*) characteristics of Ni/*p*-GaN Schottky diodes at 300 K. The fitting curve using the TFE model is also shown in Fig. 1. Yu *et al.*<sup>7</sup> indicated that the slope of  $\ln I$ –*V* curves could not be analyzed using the thermionic emission (TE) model, due to the carrier transport with a tunnel component. In addition, these reports<sup>13,14</sup> provide theoretical analysis of current tunneling through a Schottky barrier ( $q\phi_B$ ). The *J*–*V* characteristic in the presence of tunneling can be described by the relation<sup>13,14</sup>

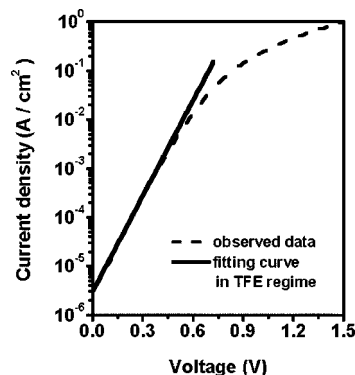


FIG. 1. *J*–*V* curve of Ni/*p*-GaN Schottky diodes under forward bias condition at 300 K and the fitting curve to the *J*–*V* characteristic in the TFE regime.

<sup>a)</sup>Electronic mail: r2r2390@yahoo.com.tw

$$J = J_0 \exp(qV/E_0), \quad (1)$$

$$E_0 = E_{00} \coth(E_{00}/kT), \quad (2)$$

$$J_0 = \frac{A^* T [\pi E_{00} q (\phi_B - V - \xi)]^{0.5}}{k \cosh(E_{00}/kT)} \exp \left[ -\frac{q\xi}{kT} - \frac{q}{E_0} (\phi_B - \xi) \right], \quad (3)$$

$$E_{00} = (qh/4\pi)(N/m^* \varepsilon)^{0.5}, \quad (4)$$

where  $J$  is the observed current density of Schottky diodes under forward bias condition,  $m^*$  ( $m^*=0.6m_0$ ,  $m_0$  is the mass of hole at rest)<sup>15</sup> is the hole effective mass,  $\varepsilon$  ( $\varepsilon=9.5\varepsilon_0$ ,  $\varepsilon_0$  is the permittivity in vacuum)<sup>16</sup> is the dielectric constant of GaN,  $A^*$  ( $A^*=103.8 \text{ A/cm}^2 \text{ K}^2$ )<sup>17</sup> is the effective Richardson constant of  $p$ -GaN,  $h$  is Planck's constant,  $V$  is voltage,  $q$  is the electron charge,  $N$  is the doping concentration, and  $\xi$  is equal to  $(E_F - E_V)/q$ .  $E_V$  is the valence band maximum and  $E_F$  is the position of the Fermi level.  $\xi$  was assumed to be equal to 0.1 V in this study. According to the fitting  $J$  versus  $V$  curve of samples using Eqs. (1)–(3), the value of  $E_0$ ,  $E_{00}$ , and  $q\phi_B$  can be calculated to be 66 meV, 65 meV, and 1.8 eV, respectively. Then, the calculated value ( $\sim 7 \times 10^{19} \text{ cm}^{-3}$ ) of  $N$  using Eq. (4) is similar to [Mg], which indicated that the tunneling current under forward bias conditions took place because of the high Mg doping [or the deep level defect (DLD) band induced by high Mg doping].<sup>18,19</sup> Kwak *et al.*<sup>18</sup> have suggested that the current transport at the metal/high Mg doped  $p$ -GaN interface was dominated by a DLD band which was induced by high Mg doping. Kwak *et al.*<sup>19</sup> have also suggested that the DLD band had a large density defect, over  $10^{19} \text{ cm}^{-3}$  size, existing in the  $p$ -GaN films and that the density of the DLDs increased as [Mg] increased. In addition, Shiojima *et al.*<sup>20</sup> have found carrier capture and emission from acceptor-like DLDs for Ni/ $p$ -GaN Schottky diodes. Further, it is worth noting that the calculated value of  $E_{00}/kT$  is slightly larger than 1, which implies the current transport processes a tunnel component.<sup>14</sup> On the other hand, the observed current is too small to obtain the fitting parameters for the  $J$ - $V$  characteristic in the field emission (FE) regime for Ni/ $p$ -GaN. This suggests that the FE model cannot be used to study the  $q\phi_B$  of Ni/ $p$ -GaN in this case. In addition, the  $E_{00}$  of 65 meV is not much greater than  $kT$  ( $kT=26 \text{ meV}$ , at 300 K), so the FE will not take place.<sup>13</sup> The effective resistance of the Schottky barrier in the FE regime is quite low, so the FE model is often used for ohmic contact.<sup>13</sup>

Figure 2 shows the typical semilog  $J$ - $V$  characteristics of Ni/ $p$ -GaN Schottky diodes at 350 and 400 K, respectively. The fitting curves using the TFE model are also shown in Fig. 2. We find that the barrier heights can readily be obtained by fitting the  $J$ - $V$  curves using Eqs. (1)–(3). From the TFE theory, a linear fit to the data for the  $J$ - $V$  measurements at 350 K yields  $E_0=67 \text{ meV}$  and  $q\phi_B=1.8 \text{ eV}$ , whereas a linear fit to the data for the  $J$ - $V$  measurements at 400 K yields  $E_0=68 \text{ meV}$  and  $q\phi_B=1.8 \text{ eV}$ . Both values for the Schottky barrier height are in good agreement with the value calculated for  $J$ - $V$  measurements at 300 K. These results indicate that a TFE model can quantitatively explain the observed large forward leakage currents due to the existence of the induced high density of the acceptor-type DLDs by

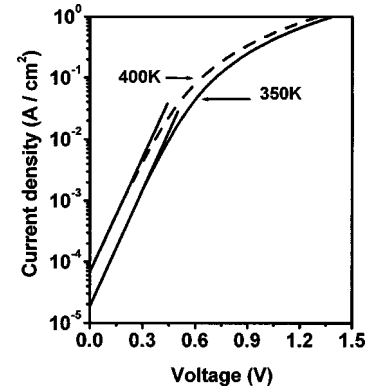


FIG. 2. Forward  $J$ - $V$  characteristic of Ni/ $p$ -GaN Schottky diodes as a function of temperature.

high Mg doping. We conclude that the creation of a large number of DLDs in  $p$ -GaN leads to the reduction of the depletion layer width in the  $p$ -GaN near the interface, an increase in the probability of the TFE, and gives rise to large forward leakage. Consequently, the forward current transport with a tunnel component is not analyzed using the TE model.

In order to further confirm whether the barrier-height value of Ni/ $p$ -GaN Schottky diodes is 1.8 eV or not, XPS is used to study the surface Fermi level position within the band gap for Ni overlayer on  $p$ -GaN. XPS measurements were performed using a monochromatic Al  $K_{\alpha}$  x-ray source. The barrier height was determined from the XPS data using the following relation.<sup>21,22</sup> This equation was previously employed by Tracy *et al.*<sup>23</sup> for the calculation of the barrier heights ( $q\phi_n$ ) of metals on  $n$ -GaN:

$$q\phi_n = E_G - E^i_v + (E^i_{\text{core}} - E^m_{\text{core}}) = E_G - (E^m_{\text{core}} - E_{VC}) \quad (5)$$

$E_G$  is the band gap of the semiconductor,  $E^m_{\text{core}}$  is the binding energy of the semiconductor core-level peak following metal deposition,  $E^i_{\text{core}}$  is the initial binding energy of the core-level peak,  $E^i_v$  is the initial binding energy of the  $E_V$  of the semiconductor, and  $E_{VC}$  is equal to  $(E^i_{\text{core}} - E^i_v)$ . All binding energies are measured relative to the  $E_F$ . For the calculation of the barrier heights ( $q\phi_p$ ) of Ni/ $p$ -GaN, the equation is expressed as

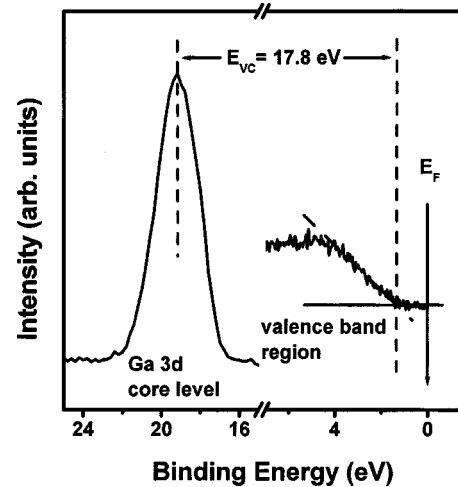


FIG. 3. The left-hand spectrum shows the Ga 3d core-level peak on  $p$ -GaN without a Ni overlayer. The right-hand panel presents the spectrum of the valence-band region. A linear fit is used to determine the energy of the valence-band edge.

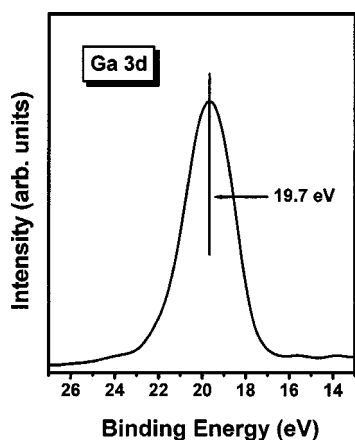


FIG. 4. Ga 3d core level at the Ni/p-GaN interface. The binding energy is referenced to the Fermi level.

$$q\phi_p = E_{\text{core}}^{\text{Ni}} - E_{\text{VC}} \quad (6)$$

where  $E_{\text{core}}^{\text{Ni}}$  is the binding energy of the  $p$ -GaN core-level peak following Ni deposition.

Figure 3 shows an example of the Ga 3d core level and the valence-band spectrum collected on a  $p$ -GaN sample without a Ni overlayer. The  $E_{\text{VC}}$  is calculated to be 17.8 eV. This value is in good agreement with the value of 17.8 eV reported by Hashizume *et al.*,<sup>24</sup> Bermudez,<sup>25</sup> Waldrop and Grant,<sup>26</sup> and Wu and Kahn.<sup>27</sup> Figure 4 shows the Ga 3d core level at the Ni/p-GaN interface. The spectra determine the Ga 3d binding energy  $E_{\text{core}}^{\text{Ni}}$  relative to the  $E_{\text{F}}$ . In Fig. 4, we can see that the  $E_{\text{core}}^{\text{Ni}}$  is equal to 19.7 eV. Therefore, the  $q\phi_p$  was calculated to be 1.9 eV, according to Eq. (6). This value is similar to the value of 1.8 eV obtained from  $J$ - $V$  measurements. In addition, Rickert *et al.*<sup>28</sup> suggested that the barrier height value of the Ni/p-GaN sample is approximately 1.9 eV, which supported our observed results from the XPS and  $J$ - $V$  measurements.

In summary, the barrier height value of Ni/p-GaN Schottky diodes was obtained from  $J$ - $V$  measurements in this study. For Ni/p-GaN Schottky diodes, the calculated barrier height value using the TFE model is in good agreement with the value of 1.9 eV obtained from x-ray photoelectron spectroscopy measurements. The induced DLD band through high Mg doping would lead to the reduction of the depletion layer width in the  $p$ -GaN near the interface, an increase in the probability of the TFE, and an increase in

current flow under forward bias conditions, which was not analyzed using the TE model.

This project is supported by National Science Council of Taiwan, Republic of China, under Contract No. NSC 93-2215-E-018-005. The XPS was kindly provided from the NTU Instrumentation Center at Taipei National Taiwan University.

<sup>1</sup>O. Katz, V. Garber, B. Meyler, G. Bahir, and J. Salzman, Appl. Phys. Lett. **79**, 1417 (2001).

<sup>2</sup>M. A. Khan, J. N. Kuznia, D. T. Olson, M. Blasingame, and A. R. Bhattarai, Appl. Phys. Lett. **63**, 2455 (1993).

<sup>3</sup>M. A. Khan, J. N. Kuznia, A. R. Bhattarai, and D. T. Olson, Appl. Phys. Lett. **62**, 1786 (1993).

<sup>4</sup>N. Biyikli, O. Aytur, I. Kimukin, T. Tut, and E. Ozbay, Appl. Phys. Lett. **81**, 3272 (2002).

<sup>5</sup>M. W. Wang, J. O. McCaldin, J. F. Swenberg, T. C. McGill, and R. J. Hauenstein, Appl. Phys. Lett. **66**, 1974 (1995).

<sup>6</sup>T. Mori, T. Kozawa, T. Ohwaki, Y. Taga, S. Naagai, S. Yamasaki, S. Asami, N. Shibata, and M. Koike, Appl. Phys. Lett. **69**, 3537 (1996).

<sup>7</sup>L. S. Yu, D. Qiao, L. Jia, S. S. Lau, Y. Qi, and K. M. Lau, Appl. Phys. Lett. **79**, 4536 (2001).

<sup>8</sup>X. A. Cao, S. J. Pearton, G. Dang, A. P. Zhang, F. Ren, and J. M. Van Hove, Appl. Phys. Lett. **75**, 4130 (1999).

<sup>9</sup>P. J. Hartlieb, A. Roskowski, R. F. Davis, W. Platow, and R. J. Nemanich, J. Appl. Phys. **91**, 732 (2002).

<sup>10</sup>D. L. Hibbard, R. W. Chuang, Y. S. Zhao, C. L. Jensen, H. P. Lee, Z. J. Dong, R. Shih, and M. Bremser, J. Electron. Mater. **29**, 291 (2000).

<sup>11</sup>K. Shiojima, T. Sugahara, and S. Sakai, Appl. Phys. Lett. **74**, 1936 (1999).

<sup>12</sup>J. K. Ho, C. S. Jong, C. N. Huang, C. C. Chiu, K. K. Shih, L. C. Chen, F. R. Chen, and J. J. Kai, J. Appl. Phys. **86**, 4491 (1999).

<sup>13</sup>Michael Shur, *Physics of Semiconductor Devices* (Prentice-Hall, Englewood Cliffs, NJ, 1990).

<sup>14</sup>H. Morkoç, *Nitride Semiconductors and Devices* (Springer, Berlin, 1999).

<sup>15</sup>C. Merz, M. Kunzer, U. Kaufmann, I. Akasaki, and H. Amano, Semicond. Sci. Technol. **11**, 712 (1996).

<sup>16</sup>M. Razeghi and A. Rogalski, J. Appl. Phys. **79**, 7433 (1996).

<sup>17</sup>J. I. Pankove, S. Bloom, and G. Harbecke, RCA Rev. **36**, 163 (1975).

<sup>18</sup>J. S. Kwak, O. H. Nam, and Y. Park, Appl. Phys. Lett. **80**, 3554 (2002).

<sup>19</sup>J. S. Kwak, O. H. Nam, and Y. Park, J. Appl. Phys. **95**, 5917 (2004).

<sup>20</sup>K. Shiojima, T. Sugahara, and S. Sakai, Appl. Phys. Lett. **77**, 4353 (2000).

<sup>21</sup>J. R. Waldrop and R. W. Grant, Appl. Phys. Lett. **52**, 1794 (1988).

<sup>22</sup>J. R. Waldrop and R. W. Grant, Appl. Phys. Lett. **62**, 2685 (1993).

<sup>23</sup>K. M. Tracy, P. J. Hartlieb, S. Einfeldt, F. Davis, E. H. Hurt, and R. J. Nemanich, J. Appl. Phys. **94**, 3939 (2003).

<sup>24</sup>T. Hashizume, S. Ootomo, S. Oyama, M. Konishi, and H. Hasegawa, J. Vac. Sci. Technol. B **19**, 1675 (2001).

<sup>25</sup>V. M. Bermudez, J. Appl. Phys. **80**, 1190 (1996).

<sup>26</sup>J. R. Waldrop and R. W. Grant, Appl. Phys. Lett. **68**, 2879 (1996).

<sup>27</sup>C. I. Wu and A. Kahn, J. Appl. Phys. **86**, 3209 (1999).

<sup>28</sup>K. A. Rickert, A. B. Ellis, J. K. Kim, J. L. Lee, F. J. Himpsel, F. Dwikusuma, and T. F. Kuech, J. Appl. Phys. **92**, 6671 (2002).



# Effect of reactive ion etching-induced defects on the surface band bending of heavily Mg-doped *p*-type GaN

Yow-Jon Lin<sup>a)</sup> and Yow-Lin Chu

*Institute of Photonics, National Changhua University of Education, Changhua 500, Taiwan, Republic of China*

(Received 16 August 2004; accepted 25 February 2005; published online 29 April 2005)

The effect of reactive ion etching-induced defects on the surface band bending of heavily Mg-doped *p*-type GaN (*p*-GaN) was investigated in this study. According to the observed results from x-ray photoelectron spectroscopy and secondary-ion-mass spectroscopy (SIMS) measurements, we found that the formation of more nitrogen-vacancy-related defects created near the surface by reactive ion etching technique would lead to an increase in the surface band bending, a shift of the surface Fermi level toward the conduction-band edge, the reduction of the current flow at the metal/etched *p*-GaN interface, and an increase in the barrier height at the metal/etched *p*-GaN interface. In addition, from the SIMS measurements, it is suggested that the depth of the nitrogen-deficient near-surface region resulting from the dry-etch process is about 60 nm. © 2005 American Institute of Physics. [DOI: 10.1063/1.1894580]

## I. INTRODUCTION

The recent progress in GaN-based optoelectronic devices, such as blue light-emitting diodes (LEDs) and laser diodes (LDs),<sup>1–3</sup> points to the need of a deeper understanding of the optical and electrical characteristics of Mg-doped *p*-type GaN (*p*-GaN). An important area in dry etching is the characterization of damage which is produced in the semiconductor through the bombardment of energetic ions. This induced damage, which may exist as vacancy complexes, dislocations, and recombination centers, can degrade the optical and electrical performances of devices. However, very little work has been done in investigating dry etch-induced defects in respect to heavily Mg-doped *p*-GaN. In this article, we report the findings from a study of the effect of reactive ion etching-induced defects on the electrical properties of heavily Mg-doped *p*-GaN. We find that according to the observed result from x-ray photoelectron spectroscopy (XPS) and secondary-ion-mass spectroscopy (SIMS) measurements, the nitrogen-vacancy-related defects induced by the reactive ion etching (RIE) technique will lead to an increase in surface band bending and a shift of the surface Fermi level toward the conduction-band edge. In addition, from the SIMS measurements, it is suggested that the depth of the nitrogen-deficient near-surface region resulting from a dry-etch process is about 60 nm. Upon *p*-type doping, the changed donor defect formation energy will decrease in tandem with the Fermi-level ( $E_F$ ) position.<sup>4,5</sup> The nitrogen-vacancy-related defect is easily formed in the *p*-GaN films and the native defect of *p*-GaN.<sup>4</sup> According to the theoretical predictions,<sup>6</sup> the only native defect with a relevant concentration in *p*-GaN is the nitrogen-vacancy-related defect.<sup>7</sup> As a result, we deduce that further nitrogen-vacancy-related defects may exist in the *p*-GaN near-surface region following etching. Another goal of this paper is to show that the RIE

represents a suitable technique choice for the fabrication of heavily Mg-doped *p*-GaN Schottky diodes with good qualities.

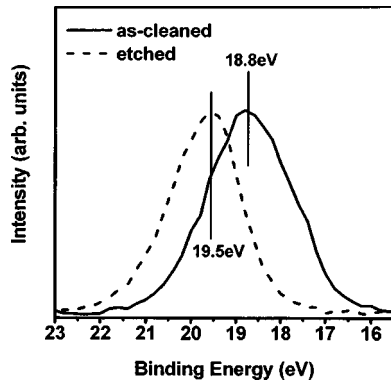
## II. EXPERIMENTAL PROCEDURE

The epitaxial layers used in the experiments were grown on *c*-plane sapphire substrates using a metal-organic chemical-vapor deposition system. Trimethylgallium, ammonia, and bis(cyclopentadienyl)magnesium were used as the Ga, N, and Mg sources, respectively. An undoped GaN buffer layer with a thickness of 650 nm was grown on the sapphire substrate at 520 °C, followed by the growth of a Mg-doped GaN layer (762 nm,  $3.6 \times 10^{17} \text{ cm}^{-3}$ ) at 1100 °C. The grown samples were annealed for the purpose of generating holes, at 750 °C for 30 min in  $\text{N}_2$  ambient. The Mg concentration ( $[\text{Mg}]$ ) was  $6 \times 10^{19} \text{ cm}^{-3}$  for all samples. The  $[\text{Mg}]$  in Mg-doped GaN was measured using SIMS. The samples were cleaned in chemical clean solutions of trichloroethylene, acetone, and methanol (referred to as as-cleaned *p*-GaN). Then, some of the as-cleaned samples were etched using the RIE technique in  $\text{BCl}_3$  plasma with a rf power of 150 W. During the etching process, the  $\text{BCl}_3$  flow rate was 5 SCCM (standard cubic centimeter per minute) and the chamber pressure was 4 Pa. The etched depth is 100 nm. The etched sample was referred to as etched *p*-GaN. The as-cleaned and etched samples were then inserted into the vacuum chamber of a ESCA PHI 1600 system. We took a Au  $4f_{7/2}$  peak and a Cu  $2p_{3/2}$  peak for energy reference purposes.

## III. EXPERIMENTAL RESULTS AND DISCUSSION

Figure 1 shows the Ga 3*d* core-level XPS spectra on the as-cleaned and etched *p*-GaN surfaces. We found that the Ga 3*d* core-level spectra of the etched sample shift toward the high binding-energy side, compared with that of the as-cleaned one. This indicated that the Ga 3*d* core-level spectra of the as-cleaned sample after etching treatment underwent a

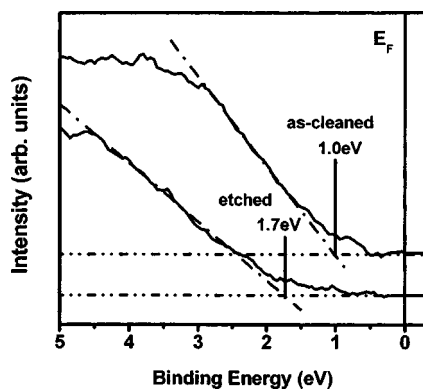
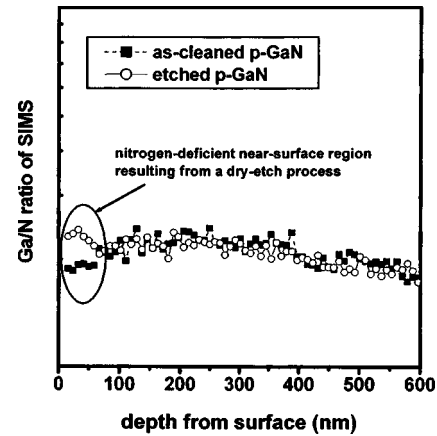
<sup>a)</sup>Author to whom correspondence should be addressed; electronic mail: rzt2390@yahoo.com.tw

FIG. 1. Ga 3d core-level XPS spectra of as-cleaned and etched *p*-GaN.

shift of 0.7 eV, and that the etching treatment gave rise to a shift of the surface Fermi level toward the conduction-band edge, resulting in an increase in the surface band bending.<sup>8,9</sup> In Fig. 1, we also found that the full width at half maximum in the Ga 3d spectra of as-cleaned *p*-GaN is slightly larger than that of etched *p*-GaN. This may be due to the fact that the contaminant and residual oxides on the *p*-GaN surface were removed during the etching process.

Figure 2 shows the XPS spectra of the as-cleaned and etched *p*-GaN surface near the valence-band edge region. The valence-band maximum (VBM) is defined in a standard way by the linear extrapolation of the low binding-energy edge of the valence-band spectrum. In Fig. 2, we can see that the VBM of the as-cleaned and etched samples is found at 1.0 and 1.7 eV below the  $E_F$ , respectively. In addition, for the as-cleaned or etched samples, the binding energy of the Ga 3d core level (18.8 eV for the as-cleaned sample and 19.5 eV for the etched sample, as shown in Fig. 1) with respect to the VBM is 17.8 eV, which is in good agreement with previous results.<sup>10,11</sup>

To investigate the characteristics of defects induced by RIE technique, the as-cleaned and etched *p*-GaN surfaces were measured using XPS quantitative analysis. The relative Ga/N atomic concentration ratio was determined from the integration of Ga 3d and N 1s peaks. In this work, the exact sensitivity factor for *p*-GaN was not known, so the Ga/N ratio on the as-cleaned *p*-GaN surface was taken as 1. Consequently, the Ga/N ratio on the etched *p*-GaN surface was calculated to be 1.5. XPS surface analysis revealed a lower

FIG. 2. XPS spectra of the as-cleaned and etched *p*-GaN surface near the valence-band edge region.FIG. 3. Depth profiles of Ga/N ratios of the as-cleaned and etched *p*-GaN samples.

nitrogen atomic concentration on the etched sample. This indicates that the RIE technique may create more nitrogen vacancies on the sub-*p*-GaN surface. The nitrogen-vacancy-related defect level above the  $E_F$ , which is near the conduction-band edge,<sup>12,13</sup> will ionize and the nitrogen-vacancy-related defects will become the dominant positively charged donors in the etched sample. For the preservation of the charge neutrality on the etched *p*-GaN surface, an increase in the positive charge for the extrinsic nitrogen-vacancy defects will lead to an increase in the negative charge in the surface space-charge region, an increase in the surface band bending, and a shift of the surface Fermi level toward the conduction-band edge. On the other hand, it has been shown that reactive ion etching *n*-type GaN surface improves the contact resistance,<sup>14</sup> which can be attributed to the formation of extrinsic donor-type nitrogen-vacancy-related defects. The suggestion is consistent with the above result of XPS analysis. Besides, we found that the reduction of the surface state, related to nitrogen-vacancy defects on the *p*-GaN surface, led to a reduction in the surface band bending by 0.25 eV in a previous study.<sup>15</sup> In contrast, more nitrogen-vacancy-related defects created near the surface by the RIE technique will lead to an increase in the surface band bending of *p*-GaN.

Figure 3 shows the depth profiles of Ga/N ratios of as-cleaned *p*-GaN and etched *p*-GaN, respectively. The intensity of Ga SIMS divided by that of N SIMS equals the Ga/N ratio. In Fig. 3, we find that the Ga/N ratio of etched samples is larger than that of as-cleaned samples in the near-surface region. This implies that more nitrogen-vacancy-related defects were formed in the etched *p*-GaN films. We also find that the depth of the nitrogen-deficient near-surface region resulting from a dry-etch process is about 60 nm. The value is in good agreement with the value of 40–60 nm reported by Cao *et al.*<sup>16</sup> and Kent *et al.*<sup>17</sup>

Figure 4 shows the current–voltage ( $I$ – $V$ ) characteristics of Ni/Au (20/20 nm, deposition used an electron-beam evaporator) contacts on as-cleaned and etched *p*-GaN. The gap spacing of the Ni/Au metals pads is 25  $\mu$ m. These  $I$ – $V$  characteristics were observed using the transmission line method (TLM). The fabrication process of the TLM pattern has been reported previously.<sup>18</sup> The  $I$ – $V$  characteristics of



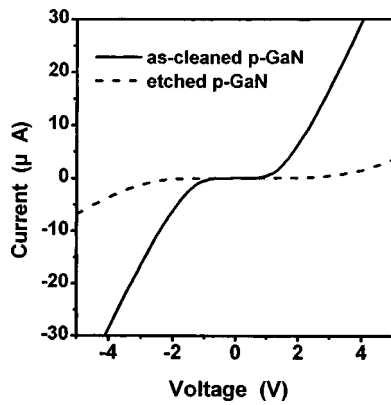


FIG. 4.  $I$ - $V$  characteristics of Ni/Au contacts on as-cleaned and etched  $p$ -GaN.

the TLM patterns were measured using a Keithley Model-4200-SCS/F semiconductor characterization system. Comparing the  $I$ - $V$  curves shown in Fig. 4, the  $I$ - $V$  curve for the as-cleaned sample is better than that of the etched sample. In addition, the  $I$ - $V$  curve for the as-cleaned sample, with a smaller turn on voltage and larger slope, is superior to that of the etched sample. The worse performance of the etched samples is attributable to the formation of the higher barrier between the Ni/Au and  $p$ -GaN and an increase in the nitrogen-vacancy-related defects, suppressing an effect of the acceptorlike deep level defects<sup>19</sup> (DLDs) on the carrier transport at the Ni/heavily Mg-doped GaN interfaces, as well as the reduction of the hole concentration and the probability of the tunneling transmission through the DLD band for holes at the metal/ $p$ -GaN interface.<sup>19,20</sup> The explanation for this is given later. Besides, in Figs. 1 and 2, we can see that the downward surface band bending of the etched samples indeed increases. This indirectly implies that an increase in the surface band bending can lead to the degradation in the  $I$ - $V$  characteristics of the etched sample. In this regard, the dry etching technique can be applied in the fabrication process of  $p$ -GaN Schottky diodes, because more nitrogen-vacancy-related defects formed below the  $p$ -GaN surface lead to an increased Schottky barrier for the transport of holes.

For Schottky diodes, secure ohmic contacts help to obtain the actual Schottky characteristics. Kwak *et al.* suggested that high Mg doping would lead to the formation of secure ohmic contacts of metals/ $p$ -GaN.<sup>19</sup> In order to obtain the good qualities of  $p$ -GaN Schottky diodes, the heavily Mg-doped  $p$ -GaN has to be used to form the low-resistivity ohmic contact. Nevertheless, Kwak *et al.* found that the current transport at the metal/high Mg-doped  $p$ -GaN interface was dominated by a deep level defect band which was induced by high Mg doping.<sup>19</sup> Kwak *et al.* suggested that the DLD band possesses a large defect density over  $10^{19}$  cm<sup>-3</sup> existing in the  $p$ -GaN films, and that the density of the DLDs was enlarged as [Mg] increased.<sup>20</sup> In addition, Shiojima *et al.*<sup>21</sup> found carrier capture and emission from acceptorlike DLDs for Ni/ $p$ -GaN Schottky diodes. According to these results reported by Kwak *et al.* and Shiojima *et al.*,<sup>19-21</sup> we deduced that the heavily Mg-doped  $p$ -GaN used to fabricate the Schottky diodes might lead to the formation of the low barrier height and a larger leakage of current at the Schottky

metals/ $p$ -GaN interface. On the basis of this evidence, we concluded that the regions of Schottky contacts of high Mg-doped  $p$ -GaN could be etched by the RIE technique after the formation of good ohmic contacts, and more nitrogen-vacancy-related defects were produced in  $p$ -GaN near the surface, suppressing an effect of the acceptorlike DLDs on  $p$ -GaN Schottky diodes. Therefore, following the deposition of metals on the etched Schottky contacts of heavily Mg-doped  $p$ -GaN samples, we expect that the higher barrier height and smaller leakage current will be easily obtained. This will be further investigated in the future. Finally, we predict that the application of the RIE technique in the fabrication of  $p$ -GaN Schottky diodes will result in the formation of a high barrier height and a smaller leakage of current at the interfaces.

#### IV. CONCLUSIONS

In summary, the effect of defects created by the RIE technique on the electrical properties of heavily Mg-doped  $p$ -GaN has been investigated. We found that the formation of more nitrogen-vacancy-related defects created near the surface by the RIE technique would lead to an increase in the downward band bending. This indicates that the etching treatment gives rise to a shift of the surface Fermi level toward the conduction-band edge, which is in good agreement with the observed result from the measurements of the valence-band spectrum. Dry etching could be useful for the formation of the high barrier height and the low leakage of current at the metals/heavily Mg-doped  $p$ -GaN interface. This fact offers hope for the application of the RIE technique in the fabrication process of heavily Mg-doped  $p$ -GaN Schottky diodes with good qualities. We plan to experimentally fabricate such Schottky diodes in the near future.

#### ACKNOWLEDGMENT

This project is supported by National Science Council of Taiwan, Republic of China, under Contract No. NSC 93-2215-E-018-005.

- <sup>1</sup>M. Osinski, *Gallium-Nitride-based Technologies* (SPIE, Washington, 2002).
- <sup>2</sup>S. J. Pearton, J. C. Zolper, R. J. Shul, and F. Ren, *J. Appl. Phys.* **86**, 1 (1999).
- <sup>3</sup>H. Morkoç, *Nitride Semiconductors and Devices* (Springer, Berlin, 1999).
- <sup>4</sup>J. Neugebauer and C. G. Van de Walle, *Phys. Rev. B* **50**, 8067 (1994).
- <sup>5</sup>S. G. Lee and K. J. Chang, *Semicond. Sci. Technol.* **14**, 138 (1999).
- <sup>6</sup>J. Neugebauer and C. G. Van de Walle, *Mater. Res. Soc. Symp. Proc.* **395**, 645 (1996).
- <sup>7</sup>U. Kaufmann, M. Kunzer, M. Maier, H. Obloh, A. Ramakrishnan, B. Santic, and P. Schlotter, *Appl. Phys. Lett.* **72**, 1326 (1998).
- <sup>8</sup>K. A. Rickert, A. B. Ellis, F. J. Himpsel, J. Sun, and T. F. Kuech, *Appl. Phys. Lett.* **80**, 204 (2002).
- <sup>9</sup>G. Landgren, R. Ludeke, Y. Jugnet, J. F. Morar, and F. J. Himpsel, *J. Vac. Sci. Technol. B* **2**, 351 (1984).
- <sup>10</sup>C. I. Wu and A. Kahn, *J. Appl. Phys.* **86**, 3209 (1999).
- <sup>11</sup>T. Hashizume, S. Ootomo, S. Oyama, M. Konishi, and H. Hasegawa, *J. Vac. Sci. Technol. B* **19**, 1675 (2001).
- <sup>12</sup>C. G. Van de Walle, in *Properties of Gallium Nitride and Related Semiconductors*, edited by J. H. Edgar, S. Strite, I. Akasaki, H. Amano, and C. Wetzel (INSPEC, London, 1999), p. 275.
- <sup>13</sup>T. L. Tansley and R. J. Egan, *Phys. Rev. B* **45**, 10942 (1992).
- <sup>14</sup>Z. Fan, S. N. Mohammad, W. Kim, O. Aktas, A. E. Botchkarev, and H. Morkoç, *Appl. Phys. Lett.* **68**, 1672 (1996).

- <sup>15</sup>Y. J. Lin, Z. L. Wang, and H. C. Chang, Appl. Phys. Lett. **81**, 5183 (2002).
- <sup>16</sup>X. A. Cao *et al.*, MRS Internet J. Nitride Semicond. Res. **5S1**, W10.8 (2000).
- <sup>17</sup>D. G. Kent *et al.*, Solid-State Electron. **45**, 467 (2001).
- <sup>18</sup>Y. J. Lin, Z. D. Li, C. W. Hsu, F. T. Chien, C. T. Lee, S. T. Shao, and H. C. Chang, Appl. Phys. Lett. **82**, 2817 (2003).
- <sup>19</sup>J. S. Kwak, O. H. Nam, and Y. Park, Appl. Phys. Lett. **80**, 3554 (2002).
- <sup>20</sup>J. S. Kwak, O. H. Nam, and Y. Park, J. Appl. Phys. **95**, 5917 (2004).
- <sup>21</sup>K. Shiojima, T. Sugahara, and S. Sakai, Appl. Phys. Lett. **77**, 4353 (2000).

# Optical and electrical properties of heavily Mg-doped GaN upon $(\text{NH}_4)_2\text{S}_x$ treatment

Yow-Jon Lin<sup>a)</sup> and Yow-Lin Chu

*Institute of Photonics, National Changhua University of Education, Changhua 500, Taiwan, Republic of China*

Y. S. Huang

*Department of Electronic Engineering, National Taiwan University of Science and Technology, Taipei 106, Taiwan, Republic of China*

Hsing-Cheng Chang

*Department of Automatic Control Engineering, Feng Chia University, Taichung 407, Taiwan, Republic of China*

(Received 12 January 2005; accepted 29 March 2005; published online 10 May 2005)

We have employed the photoluminescence (PL) and surface photovoltage spectroscopy (SPS) measurements to study the effects of  $(\text{NH}_4)_2\text{S}_x$  treatment on the optical and electrical properties of  $p$ -type GaN ( $p$ -GaN) in this study. From the PL and SPS measurements, it is suggested that the  $(\text{Mg}_{\text{Ga}}-\text{V}_{\text{N}})^{2+}$  ( $\text{Mg}_{\text{Ga}}$ : Ga vacancies occupied by Mg;  $\text{V}_{\text{N}}$ : nitrogen vacancies) complexes near the  $p$ -GaN surface region were transformed into the  $(\text{Mg}_{\text{Ga}}-\text{S}_{\text{N}})^0$  ( $\text{S}_{\text{N}}$ : N vacancies occupied by S) complexes after  $(\text{NH}_4)_2\text{S}_x$  treatment, which resulted in the reduction of the  $\sim 2.8$ -eV PL intensity and the increase of the hole concentration near the  $p$ -GaN surface region. © 2005 American Institute of Physics. [DOI: 10.1063/1.1926404]

In recent years, GaN-related wide band gap semiconductors have become the materials of choice for the fabrication of light emitting diodes operating in the green, blue, and violet regions of the visible spectrum.<sup>1,2</sup> The fabrication of high-quality ohmic contacts on  $n$ - and  $p$ -type GaN is essential for improving the performance of optoelectronic devices. However, ohmic contact formation to  $p$ -type GaN ( $p$ -GaN) alloyed has been difficult to realize due to the absence of metals having a work function larger than that of  $p$ -GaN and the absence of  $p$ -GaN having a higher hole concentration. Recently, several groups have employed  $(\text{NH}_4)_2\text{S}_x$  treatment which was designed to improve the electrical properties of ohmic contacts to  $p$ -GaN.<sup>3–5</sup> Lee *et al.* suggested that the reduction of contact resistivity is due to direct contact of Pt on the clean  $p$ -GaN surface, via shift of barrier height for holes at the Pt/ $p$ -GaN interface.<sup>3</sup> Jang and Seong have indicated that surface treatment led to an increase in the hole concentration of  $p$ -GaN and the occurrence probability of the field emission for holes at the Pt/ $p$ -GaN interface.<sup>4</sup> However, the effect of  $(\text{NH}_4)_2\text{S}_x$  treatment on optical properties of  $p$ -GaN has not been investigated further. To date, the relationship between the optical and electrical properties of  $p$ -GaN with surface treatment has also not yet been well understood. For this study, we demonstrate that  $(\text{NH}_4)_2\text{S}_x$  treatment results in the reduction of  $\sim 2.8$ -eV photoluminescence (PL) intensity of the heavily Mg-doped  $p$ -GaN sample. We deduce that the  $(\text{Mg}_{\text{Ga}}-\text{V}_{\text{N}})^{2+}$  ( $\text{Mg}_{\text{Ga}}$ : Ga vacancies occupied by Mg,  $\text{V}_{\text{N}}$ : nitrogen vacancies) complexes near the  $p$ -GaN surface region were transformed into the  $(\text{Mg}_{\text{Ga}}-\text{S}_{\text{N}})^0$  ( $\text{S}_{\text{N}}$ : N vacancies occupied by S) complexes after  $(\text{NH}_4)_2\text{S}_x$  treatment, which led to the reduction of donor-type  $\text{V}_{\text{N}}$ -related states near the surface region and an increase in

the hole concentration.<sup>4</sup> This can explain why  $(\text{NH}_4)_2\text{S}_x$  treatment is useful for the improvement of the electrical properties of ohmic contacts to  $p$ -GaN.

The epitaxial layers used in the experiments were grown on  $c$ -plane sapphire substrates using a metal-organic chemical vapor deposition system. Trimethylgallium, ammonia and bis-cyclopentadienylmagnesium were used as the Ga, N, and Mg sources, respectively. An undoped GaN buffer layer with a thickness of 650 nm was grown on the sapphire substrate at 520 °C, followed by the growth of Mg-doped GaN layer (762 nm, Mg concentration  $= 6 \times 10^{19} \text{ cm}^{-3}$ ) at 1100 °C. The grown samples were annealed for the purpose of generating holes, at 750 °C for 30 min in  $\text{N}_2$  ambient. The samples were cleaned in chemical clean solutions of trichloroethylene, acetone, and methanol (referred to as as-cleaned  $p$ -GaN). Then, some of the as-cleaned samples were dipped into a  $(\text{NH}_4)_2\text{S}_x$  solution ( $S=6\%$ ) at 60 °C for 30 min [referred to as  $(\text{NH}_4)_2\text{S}_x$ -treated  $p$ -GaN]. The as-cleaned and  $(\text{NH}_4)_2\text{S}_x$ -treated samples were then measured via PL and surface photovoltage spectroscopy (SPS). The SPS measurements, which used normalized incident light intensity,<sup>6</sup> were performed at normal incidence using a fixed grid and probe light chopped at 200 Hz. SPS is a powerful tool for the investigation of surface electronic structure, which has proven to be an extensive source of information about optically active surface states at clean and real surfaces of various semiconductors, as well as surface with monolayer coverage.<sup>7–9</sup>

Figure 1 shows the room-temperature PL spectrum of the as-cleaned  $p$ -GaN and  $(\text{NH}_4)_2\text{S}_x$ -treated  $p$ -GaN, respectively. Using a He–Cd laser as an excitation source, the  $\sim 2.8$ -eV PL band was only observed for the all samples due to the heavily Mg doped.<sup>10</sup> According to the reported result by Kaufmann *et al.*,<sup>11</sup> we find that the generation of the  $\sim 2.8$ -eV PL band may be attributed to the  $\text{Mg}_{\text{Ga}}$  and  $\text{Mg}_{\text{Ga}}-\text{V}_{\text{N}}$  complexes. In Fig. 1, we find that the PL intensity

<sup>a)</sup> Author to whom correspondence should be addressed; electronic mail: r2r2390@yahoo.com.tw

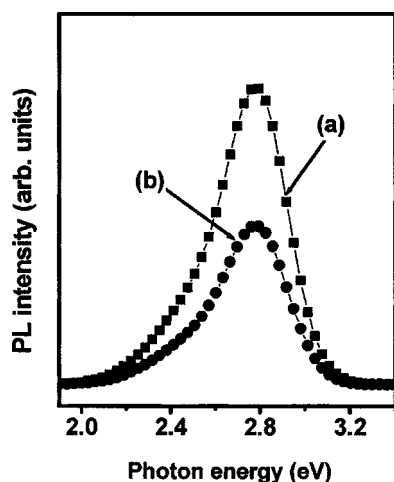


FIG. 1. Room-temperature PL spectra of (a) as-cleaned  $p$ -GaN and (b)  $(\text{NH}_4)_2\text{S}_x$ -treated  $p$ -GaN.

of the  $(\text{NH}_4)_2\text{S}_x$ -treated  $p$ -GaN is lower than that of the as-cleaned  $p$ -GaN. An explanation for this will be given later.

Figure 2 shows the room-temperature surface photovoltage (SPV) spectra of the as-cleaned and  $(\text{NH}_4)_2\text{S}_x$ -treated  $p$ -GaN samples, respectively. The slope changes indicated a one gap state, whose position relative to the conduction band minimum  $E_c$  (valence band maximum  $E_v$ ) can be deduced from the position of the downward (upward) slope changes in the spectra.<sup>12,13</sup> We can see that the upward slope change at  $\sim 3.07$  eV indicates population of a donor state, situated at  $\sim 3.07$  eV above the  $E_v$  [ $E_v + 3.07$  eV, denoted by  $D_1$  in Fig. 2(a)]. This state is attributed to the  $(\text{Mg}_{\text{Ga}}-\text{V}_{\text{N}})^{2+}$  complex.<sup>11,14</sup> Kaufmann *et al.* have suggested that the  $\text{Mg}_{\text{Ga}}-\text{V}_{\text{N}}$  complex may exist in the heavily Mg-doped  $p$ -GaN layer.<sup>15</sup> The  $\text{Mg}_{\text{Ga}}-\text{V}_{\text{N}}$  complex which is double donors resulted in the reduction of the hole concentration in the heavily Mg-doped  $p$ -GaN sample.<sup>15,16</sup> However, in Fig. 2(b), we did not find population of a donor state, situated at  $E_v + 3.07$  eV. This suggests that  $(\text{NH}_4)_2\text{S}_x$  treatment resulted in the removal of the donor-type  $(\text{Mg}_{\text{Ga}}-\text{V}_{\text{N}})^{2+}$  complexes near the  $p$ -GaN surface region. We deduce that the  $(\text{Mg}_{\text{Ga}}-\text{V}_{\text{N}})^{2+}$  complexes near the  $p$ -GaN surface region were transformed into the  $(\text{Mg}_{\text{Ga}}-\text{S}_{\text{N}})^0$  complexes after  $(\text{NH}_4)_2\text{S}_x$  treatment and the  $(\text{Mg}_{\text{Ga}}-\text{S}_{\text{N}})^0$  complex near the  $p$ -GaN surface region prefers a neutrality charged state, which results in the reduction of the observed  $\sim 2.8$ -eV PL intensity. Kim

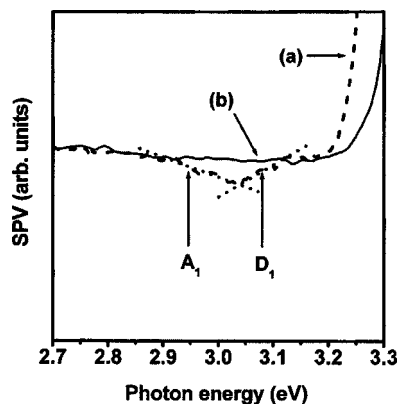


FIG. 2. Room-temperature SPV spectra of (a) as-cleaned and (b)  $(\text{NH}_4)_2\text{S}_x$ -treated  $p$ -GaN.

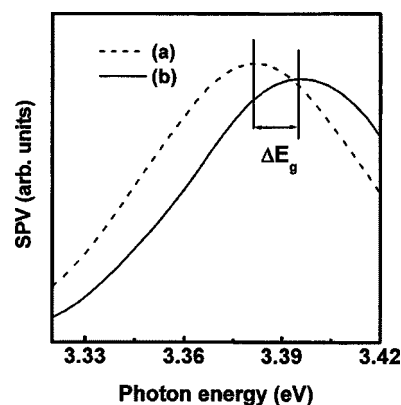


FIG. 3. Room-temperature SPV spectra of (a) as-cleaned and (b)  $(\text{NH}_4)_2\text{S}_x$ -treated  $p$ -GaN in the higher photon-energy region.

*et al.* have suggested that the reduction of  $\text{Mg}_{\text{Ga}}-\text{V}_{\text{N}}$  led to the reduction of the observed  $\sim 2.8$ -eV PL intensity.<sup>16</sup>

In a previous report,<sup>17</sup> we have demonstrated that the S atoms might occupy nitrogen-related vacancies near the  $(\text{NH}_4)_2\text{S}_x$ -treated  $p$ -GaN surface region. In addition, Oh *et al.* have suggested that PL is sensitive to material surface.<sup>18</sup> Besides, we predict that the neutral  $(\text{Mg}_{\text{Ga}}-\text{S}_{\text{N}})^0$  complex will not play the role of the compensating donor. According to the reported results by Lee *et al.*,<sup>3</sup> Jang and Seong,<sup>4</sup> and Lee *et al.*,<sup>5</sup> we find that the current-voltage characteristic of the metals/ $(\text{NH}_4)_2\text{S}_x$ -treated  $p$ -GaN sample is indeed better than that of the metals/as-cleaned  $p$ -GaN sample.<sup>5</sup> This indirectly implies that the formation the neutral  $(\text{Mg}_{\text{Ga}}-\text{S}_{\text{N}})^0$  complexes near the  $p$ -GaN surface region may lead to an increase in the hole concentration and the improvement in the electrical properties of the metals/ $(\text{NH}_4)_2\text{S}_x$ -treated  $p$ -GaN sample. A proof for this will be given later. On the other hand, we can also see that the downward slope change at 2.9–3.0 eV indicates population of an acceptor state, situated at 0.4–0.5 eV above the  $E_v$ , [denoted by  $A_1$  in Fig. 2(a)]. The acceptor state is attributed to the contamination-induced surface state (i.e., the native oxide or carbon-related contamination).<sup>19</sup> Hartlieb *et al.*<sup>19</sup> indicated that the band of surface states may extend as far as 0.6 eV above the  $E_v$ , according to the reported results by Wu and Kahn<sup>20</sup> and Bermudez.<sup>21</sup> However, the native oxide and carbon-related contamination on the  $p$ -GaN surface could be effectively removed using  $(\text{NH}_4)_2\text{S}_x$  treatment.<sup>22</sup> As a result, we do not find population of the acceptor state for  $(\text{NH}_4)_2\text{S}_x$ -treated  $p$ -GaN [shown in Fig. 2(b)].

Figure 3 shows the room-temperature SPV spectra in the higher photon-energy region. We find that the peak at 3.382 eV represents the band-to-band transition for as-cleaned  $p$ -GaN [shown in Fig. 3(a)]. Similarly, we also find that the peak at 3.396 eV represents the band-to-band transition for  $(\text{NH}_4)_2\text{S}_x$ -treated  $p$ -GaN [shown in Fig. 3(b)]. The larger band gap ( $E_g$ ) of the  $(\text{NH}_4)_2\text{S}_x$ -treated sample than that of the as-cleaned sample is found (shown in Fig. 3), due to the reduction of the gap state density during the  $(\text{NH}_4)_2\text{S}_x$  treatment.<sup>23,24</sup> This band-gap shift ( $\Delta E_g$ ) is associated with the Burstein–Moss shift and this shift energy ( $E$ ) can be written as<sup>25</sup>



$$E = E_g - E_{go} = \frac{\pi^2 h^2}{2m_r^*} \left( \frac{3N}{\pi} \right)^{2/3}, \quad (1)$$

where  $E_g$  is the transition energy gap of  $p$ -GaN,  $E_{go}$  is the intrinsic band gap of  $p$ -GaN,  $h$  is Planck's constant,  $N$  is the carrier concentration of  $p$ -GaN, and  $m_r^*$  is the reduced effective mass of  $p$ -GaN. It can be seen from Eq. (1) that an increase in  $E$  will lead to an increase in  $N$ . Kim *et al.* have indicated that the increase in band gap may be attributed to the increased carrier concentration and the increase in carrier concentration can be explained by the Burstein–Moss shift.<sup>26</sup> Lo *et al.* have also suggested that the band-gap shifts were due to the Burstein–Moss shift, which is related to the carrier concentration.<sup>27</sup> On the basis of the evidence, we deduce that the  $(\text{Mg}_{\text{Ga}}-\text{V}_{\text{N}})^{2+}$  complexes near the  $p$ -GaN surface region were transformed into the  $(\text{Mg}_{\text{Ga}}-\text{S}_{\text{N}})^0$  complexes after  $(\text{NH}_4)_2\text{S}_x$  treatment, which led to an increase in the hole concentration near the  $p$ -GaN surface region and the reduction of the  $\sim 2.8$ -eV PL intensity, which is in agreement with the reported results by Kim *et al.*<sup>16</sup>

In summary, the effects of  $(\text{NH}_4)_2\text{S}_x$  treatment on the optical and electrical properties of the heavily Mg-doped  $p$ -GaN sample were investigated. After  $(\text{NH}_4)_2\text{S}_x$  treatment, the  $(\text{Mg}_{\text{Ga}}-\text{V}_{\text{N}})^{2+}$  complexes near the  $p$ -GaN surface region were transformed into the neutral  $(\text{Mg}_{\text{Ga}}-\text{S}_{\text{N}})^0$  complexes, which led to the reduction of the donor-type states near the surface region, an increase in the hole concentration near the surface region, and the reduction of the  $\sim 2.8$ -eV PL intensity. This could explain why  $(\text{NH}_4)_2\text{S}_x$  treatment is useful for the improvement of the electrical properties of ohmic contacts to  $p$ -GaN.

This project is supported by National Science Council of Taiwan, Republic of China.

- <sup>1</sup>H. Morkoç, *Nitride Semiconductors and Devices* (Springer, Berlin, 1999).
- <sup>2</sup>S. Nakamura and S. F. Chichibu, *Introduction to Nitride Semiconductor Blue Lasers and Light Emitting Diodes* (Taylor & Francis, London, 2000).
- <sup>3</sup>J. L. Lee, J. K. Kim, J. W. Lee, Y. J. Park, and T. Kim, *Phys. Status Solidi A* **176**, 763 (1999).
- <sup>4</sup>J. S. Jang and T. Y. Seong, *Appl. Phys. Lett.* **76**, 2743 (2000).
- <sup>5</sup>C. S. Lee, Y. J. Lin, and C. T. Lee, *Appl. Phys. Lett.* **79**, 3815 (2001).
- <sup>6</sup>L. Aigouy, F. H. Pollak, J. Petruzzello, and K. Shahzad, *Solid State Commun.* **102**, 887 (1997).
- <sup>7</sup>M. Leibovitch, L. Kronik, E. Fefer, and Y. Shapira, *Phys. Rev. B* **50**, 1739 (1994).
- <sup>8</sup>Y. Rosenwaks, L. Burstein, Y. Shapira, and D. Huppert, *Appl. Phys. Lett.* **57**, 458 (1990).
- <sup>9</sup>J. Szuber, *Appl. Surf. Sci.* **55**, 143 (1992).
- <sup>10</sup>S. M. Jeong, H. W. Shim, H. S. Yoon, M. G. Cheong, R. J. Choi, E. K. Suh, and H. J. Lee, *J. Appl. Phys.* **91**, 9711 (2002).
- <sup>11</sup>U. Kaufmann, M. Kunzer, M. Maier, H. Obloh, A. Ramakrishnan, B. Santic, and P. Schlotter, *Appl. Phys. Lett.* **72**, 1326 (1998).
- <sup>12</sup>N. Kinrot and Y. Shapira, *Phys. Rev. B* **65**, 245303 (2002).
- <sup>13</sup>S. Kuźmiński, *Vacuum* **54**, 189 (1999).
- <sup>14</sup>M. A. Reshchikov, G.-C. Yi, and B. W. Wessels, *Phys. Rev. B* **59**, 13176 (1999).
- <sup>15</sup>U. Kaufmann, P. Schlotter, H. Obloh, A. Ramakrishnan, K. Köhler, and M. Maier, *Phys. Rev. B* **62**, 10867 (2000).
- <sup>16</sup>S. W. Kim, J. M. Lee, C. Huh, N. M. Park, H. S. Kim, I. H. Lee, and S. J. Park, *Appl. Phys. Lett.* **76**, 3079 (2000).
- <sup>17</sup>Y. J. Lin, C. D. Tsai, Y. T. Lyu, and C. T. Lee, *Appl. Phys. Lett.* **77**, 687 (2000).
- <sup>18</sup>E. Oh, B. Kim, H. Park, and Y. Park, *Appl. Phys. Lett.* **73**, 1883 (1998).
- <sup>19</sup>P. J. Hartlieb, A. Roskowski, R. F. Davis, W. Platow, and R. J. Nemanich, *J. Appl. Phys.* **91**, 732 (2002).
- <sup>20</sup>C. I. Wu and A. Kahn, *J. Appl. Phys.* **86**, 3209 (1999).
- <sup>21</sup>V. M. Bermudez, *J. Appl. Phys.* **80**, 1190 (1996).
- <sup>22</sup>J. K. Kim, J. L. Lee, J. W. Lee, Y. J. Park, and T. Kim, *J. Vac. Sci. Technol. B* **17**, 497 (1999).
- <sup>23</sup>W. Mönch, *J. Vac. Sci. Technol. B* **4**, 1085 (1986).
- <sup>24</sup>C. Tejedor, F. Flores, and E. Louis, *J. Phys. C* **10**, 2163 (1977).
- <sup>25</sup>S. Ray, R. Banerjee, N. Basu, A. K. Batabyal, and A. K. Barua, *J. Appl. Phys.* **54**, 3497 (1983).
- <sup>26</sup>H. Kim, A. Piqué, J. S. Horwitz, H. Mattoussi, H. Murata, Z. H. Kafafi, and D. B. Chrisey, *Appl. Phys. Lett.* **74**, 3444 (1999).
- <sup>27</sup>C. Y. Lo, C. L. Hsu, Q. X. Yu, H. Y. Lee, and C. T. Lee, *J. Appl. Phys.* **92**, 274 (2002).



# Electrical properties of Ni/Au and Au contacts on *p*-type GaN

Yow-Jon Lin<sup>a)</sup>

*Institute of Photonics, National Changhua University of Education, Changhua 500, Taiwan, Republic of China*

(Received 3 August 2004; accepted 25 October 2004; published 28 December 2004)

The electrical properties of Ni/Au and Au contacts on *p*-type GaN (*p*-GaN) were investigated in this study. From the experimental result, it is suggested that the current–voltage characteristic of Au/Ni/*p*-GaN is better than that of Au/*p*-GaN. The secondary-ion mass spectroscopy measurements revealed that hydrogen is effectively removed from the *p*-GaN layer by the existence of the Ni film. These results suggest that a Ni film of Au/Ni/*p*-GaN significantly enhances hydrogen desorption from the *p*-GaN film, which leads to an increase in the hole concentration, the occurrence of the tunneling transmission for holes at the interface, and the improvement of electrical properties of Au/Ni/*p*-GaN. © 2005 American Vacuum Society. [DOI: 10.1116/1.1835312]

## I. INTRODUCTION

GaN has drawn much interest as a promising material for the fabrication of optoelectronic devices because of the success in commercialization of blue light-emitting diodes.<sup>1–3</sup> To date, the contact resistance is not low enough to be applied for blue laser diode because there is no metal with a high work function comparable to that of *p*-GaN. In order to manufacture low-resistivity ohmic contacts, various contact schemes have been investigated.<sup>4–16</sup> In recent years, the Au/Ni/*p*-GaN ohmic contacts annealed in air have been studied extensively because they provide low specific contact resistances and high transparency.<sup>7–16</sup> Kim *et al.* concluded that the improvement of oxidized Ni/Au contact properties is due mainly to the formation of an intermediate NiO layer, rather than to an enhancement in *p*-type activation.<sup>9</sup> Qiao *et al.* indicated that the presence of oxygen during annealing appears to increase the conductivity of the *p*-GaN.<sup>10</sup> Koide *et al.* indicated that the reason for reduction of the contact resistance by the oxygen gas addition was believed to be due to formation of the *p*-GaN epilayer with high hole concentration, caused by removal of hydrogen atoms that bonded with Mg atoms.<sup>11</sup> Mistele *et al.* suggested that the layer structure of the Ni/Au layers do not seem to be that important than the selection of the annealing gas.<sup>16</sup> The previous studies<sup>7–16</sup> were focused on the effect of annealing in a partial oxygen ambient on electrical properties of ohmic contacts to *p*-GaN. To our knowledge, the formation mechanism of ohmic contacts of Au/Ni/*p*-GaN annealed under nitrogen ambient and the effects of Ni film on electrical properties of Ni/Au ohmic contacts to *p*-GaN have not yet been well understood. In this study, we find that a Ni film plays an important role in the formation of Ni/Au ohmic contacts to *p*-GaN. According to the experimental result, we deduce that a Ni layer on *p*-GaN enhances the activation of the acceptor and improves the ohmic performance of Au/Ni/*p*-GaN.

## II. EXPERIMENTAL PROCEDURES

The epitaxial layers used in the experiments were grown on *c*-plane sapphire substrates using a metalorganic chemical vapor deposition system. Trimethylgallium, ammonia (NH<sub>3</sub>), and bis-cyclopentadienylmagnesium were used as the Ga, N, and Mg sources, respectively. An undoped GaN buffer layer with a thickness of 650 nm was grown on the sapphire substrate at 520°C, followed by the growth of an *p*-GaN layer (762 nm) at 1100°C. Mg concentration ([Mg]) was  $9 \times 10^{19} \text{ cm}^{-3}$  for all samples. The [Mg] in *p*-GaN was measured using secondary-ion mass spectroscopy (SIMS). The grown samples were annealed at 750°C for 30 min in nitrogen ambient using a thermal annealing furnace for the purpose of generating holes.<sup>12</sup> The specific contact resistance was measured using the transmission line method (TLM) for Ni/Au or Au contacts to *p*-GaN. A Ni/Au (50/600 nm) metal mask was employed to form rectangular mesa regions with dimensions of  $100 \times 100 \mu\text{m}^2$ . A reactive ion etching system was used with BCl<sub>3</sub> gas to etch the *p*-GaN wafers. The dimensions of the metal contact pads in the TLM pattern was  $100 \times 100 \mu\text{m}^2$ . The gap spacings between the contact pads were designed to be 5, 10, 15, 25, 35, 50, and 60  $\mu\text{m}$ . After the removal of the metallic mask, the samples were cleaned in chemical cleaning solutions of trichloroethylene, acetone, and methanol (as-cleaned *p*-GaN). The surfaces of the as-cleaned *p*-GaN samples were treated with aqua regia for 10 min prior to respective deposition of the Ni/Au (20/20 nm) and Au (40 nm) metals using an electron-beam evaporator. Next, the contacts were treated in a rapid thermal annealing furnace at 300°C for 1 min (or 2 min) under nitrogen ambient. The current–voltage (*I*–*V*) characteristics of the TLM patterns, before and after annealing, were measured using a Keithley Model-4200-SCS/F semiconductor parameter analyzer.

## III. EXPERIMENTAL RESULTS AND DISCUSSION

Figure 1 shows the respective *I*–*V* characteristics of Au/Ni/*p*-GaN and Au/*p*-GaN, measured between metal pads with a gap spacing of 25  $\mu\text{m}$ . The Au/Ni/*p*-GaN sample does not show a linear *I*–*V* behavior. The

<sup>a)</sup>Electronic mail: r2r2390@yahoo.com.tw

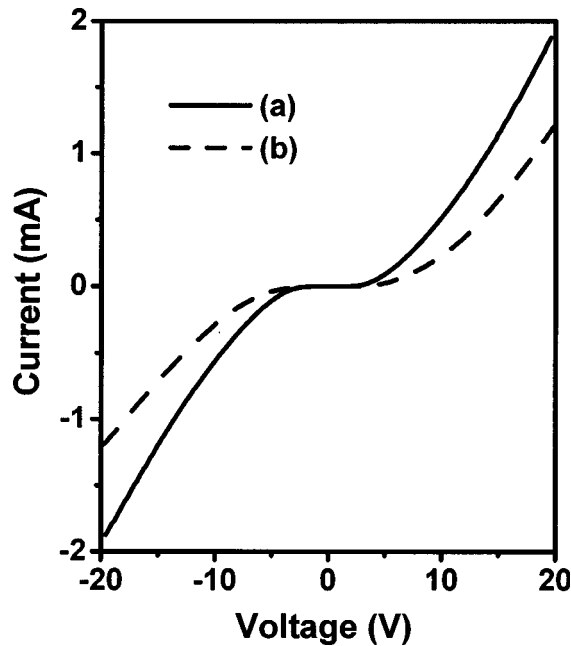


FIG. 1. Typical  $I$ - $V$  curves of (a) Au/Ni/ $p$ -GaN and (b) Au/ $p$ -GaN before annealing.

Au/ $p$ -GaN sample does not also show a linear  $I$ - $V$  curve. However, in Fig. 1, we find that the  $I$ - $V$  characteristic of the Au/Ni/ $p$ -GaN sample is better than that of the Au/ $p$ -GaN sample. On the other hand, Qiao *et al.* suggested that the Au layer has a larger work function than the Ni layer.<sup>10</sup> This implies that the contact conductivity of the Au/ $p$ -GaN sample may be higher than that of the Ni/ $p$ -GaN sample. This cannot explain why the  $I$ - $V$  characteristic of the Au/Ni/ $p$ -GaN sample is better than that of the Au/ $p$ -GaN sample. An explanation for this will be given later.

Figure 2 shows the respective  $I$ - $V$  characteristics of the annealed Au/Ni/ $p$ -GaN sample and the annealed Au/ $p$ -GaN sample, measured between metal pads with a gap spacing of 25  $\mu\text{m}$ . The Au/ $p$ -GaN samples were annealed at 300°C for 1 min in nitrogen ambient. Some of the Au/Ni/ $p$ -GaN samples were annealed at 300°C for 1 min in nitrogen ambient (1-min-annealed Au/Ni/ $p$ -GaN sample). Some of the Au/Ni/ $p$ -GaN samples were annealed at 300°C for 2 min in nitrogen ambient (2-min-annealed Au/Ni/ $p$ -GaN sample). We find that the 1-min-annealed Au/Ni/ $p$ -GaN samples show an approximate linear  $I$ - $V$  behavior with a specific contact resistance of  $7.5 \times 10^{-3} \Omega \text{ cm}^2$ . Similarly, the 2-min-annealed Au/Ni/ $p$ -GaN samples also show an approximate linear  $I$ - $V$  behavior with a specific contact resistance of  $4.2 \times 10^{-3} \Omega \text{ cm}^2$ . On the other hand, we find that the  $I$ - $V$  curve of the annealed Au/ $p$ -GaN sample is similar to that of the unannealed Au/ $p$ -GaN sample. According to the experimental result, it is suggested that a Ni film played an important role in the ohmic contact formation of Au/Ni/ $p$ -GaN.

In order to clarify the effects of the Ni film on electrical properties of the Au/Ni/ $p$ -GaN sample, we investigated the hydrogen content in the  $p$ -GaN film by SIMS measurements

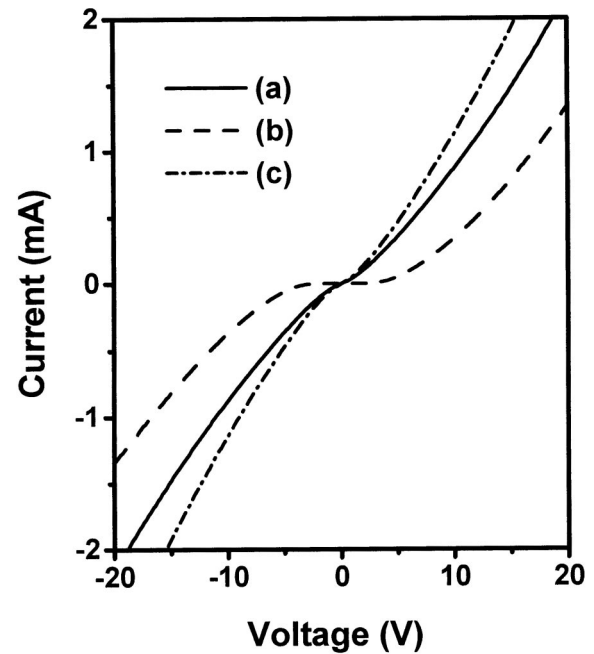


FIG. 2. Typical  $I$ - $V$  curves of (a) Au/Ni/ $p$ -GaN annealed at 300°C for 1 min, (b) Au/ $p$ -GaN annealed at 300°C for 1 min, and (c) Au/Ni/ $p$ -GaN annealed at 300°C for 2 min.

(Cameca IMS-4f system). First, Au and Ni/Au were deposited on all  $p$ -GaN surfaces. Next, these samples were annealed at 300°C for 1 min (or 2 min) in nitrogen ambient. To remove the Au (Au/Ni) film, the annealed Au/ $p$ -GaN (Au/Ni/ $p$ -GaN) samples were treated in aqua regia solution for 10 min, rinsed in deionized water for 1 min, and dried by a nitrogen blower. Next, these samples were measured using SIMS. Figure 3(a) shows the SIMS profile of hydrogen content for the as-cleaned  $p$ -GaN samples. Figure 3(b) shows the SIMS profiles of hydrogen content of Au/ $p$ -GaN annealed at 300°C for 1 min. Figure 3(c) shows the SIMS profiles of hydrogen content of Au/Ni/ $p$ -GaN annealed at 300°C for 1 min. Figure 3(d) shows the SIMS profiles of hydrogen content of Au/Ni/ $p$ -GaN annealed at 300°C for 2 min. It is noteworthy that the hydrogen content of the 1-min-annealed (or 2-min-annealed) Au/Ni/ $p$ -GaN samples is lower than that of the annealed Au/ $p$ -GaN sample or that of the as-cleaned  $p$ -GaN samples. This is in good agreement with the previous report<sup>17</sup> that the Ni film significantly enhances hydrogen desorption from the  $p$ -GaN film, which leads to an increase in the hole concentration and the improvement of electrical properties of Au/Ni/ $p$ -GaN. As a result, the Ni film enhances activation of Mg acceptors as catalysts at low temperature, causing the improvement of the electrical properties of Au/Ni/ $p$ -GaN, as shown in Figs. 1 and 2. We also find that the  $I$ - $V$  characteristic of the 2-min-annealed Au/Ni/ $p$ -GaN sample is better than that of the 1-min-annealed Au/Ni/ $p$ -GaN sample, because the hydrogen content of the 2-min-annealed Au/Ni/ $p$ -GaN sample is lower than that of the 1-min-annealed Au/Ni/ $p$ -GaN sample, as shown in Figs. 2 and 3. On the other hand, Rickert *et al.* have indicated that the barrier-height value of

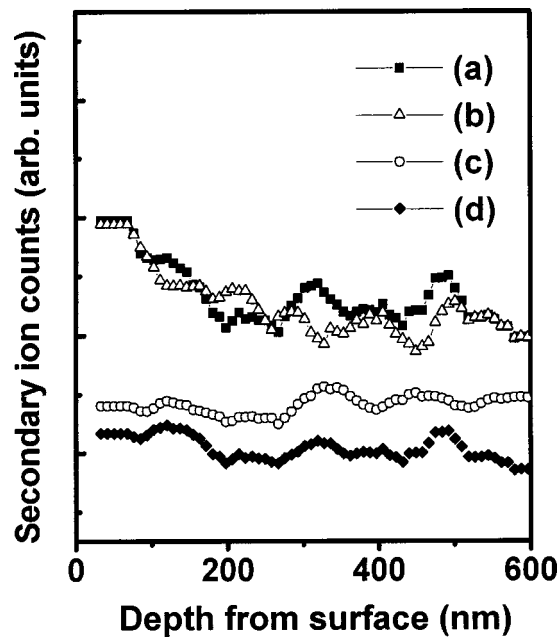


FIG. 3. SIMS profile of hydrogen content of (a) as-cleaned  $p$ -GaN, (b) Au/ $p$ -GaN annealed at 300°C for 1 min, (c) Au/Ni/ $p$ -GaN annealed at 300°C for 1 min, and (d) Au/Ni/ $p$ -GaN annealed at 300°C for 2 min.

Au/ $p$ -GaN or Ni/ $p$ -GaN is approximately equal to 1.9 eV.<sup>18</sup> Yu *et al.* have indicated that the value of tunneling parameter ( $E_{00}$ ) of unannealed Ni/ $p$ -GaN was calculated to be 0.056 eV.<sup>19</sup> The deduced value of  $E_{00}$  is likely to contain a tunneling component.<sup>19</sup> This indirectly suggests that the Ni film of Au/Ni/ $p$ -GaN absorbs hydrogen and enhances activation of Mg acceptors, causing the occurrence of the tunneling transmission for holes at the Ni/ $p$ -GaN interface. Consequently, we deduce that the selection of the Ni/Au layers seems to be an important factor for improving the ohmic contacts of  $p$ -GaN.

In Fig. 3, we can also see that the hydrogen content of the annealed Au/ $p$ -GaN sample is close to that of the as-cleaned  $p$ -GaN sample. Nakamura *et al.* have indicated that the low-resistivity  $p$ -GaN films were obtained by  $N_2$ -ambient thermal annealing above 700°C.<sup>20</sup> Nakamura *et al.* also suggested that almost no change in resistivity was observed when the  $p$ -GaN sample was annealed between room temperature and 400°C.<sup>20</sup> This implies that low-temperature activation of  $p$ -GaN and low-temperature hydrogen desorption from the  $p$ -GaN film were difficult to achieve by the absence of Ni film.

#### IV. SUMMARY

In this study, the  $I$ - $V$  characteristics of Au/Ni/ $p$ -GaN and Au/ $p$ -GaN, and the effects of Ni layer on contact resistivity of Au/Ni/ $p$ -GaN have been investigated. SIMS measurements have revealed that the Ni layer on  $p$ -GaN enhances the activation of the acceptor, as well as the occurrence of the tunneling transmission for holes at the Ni/ $p$ -GaN interface, and improves the ohmic performance of Au/Ni/ $p$ -GaN. This is probably due to the catalytic effect of Ni for the hydrogen desorption.

#### ACKNOWLEDGMENTS

The author would like to thank the National Science Council of the Republic of China for financially supporting this research under Contract No. NSC 93-2215-E-018-005. The SIMS was kindly provided from the NTHU Instrumentation Center at Hsinchu National Tsing Hua University.

<sup>1</sup>M. Osiński, *Gallium-Nitride-Based Technologies* (SPIE, Washington, 2002).

<sup>2</sup>H. Morkoç, *Nitride Semiconductors and Devices* (Springer, Berlin, 1999).

<sup>3</sup>E. F. Schubert, *Light-Emitting Diodes* (Cambridge University Press, Cambridge, 2003).

<sup>4</sup>J. S. Kwak, O. H. Nam, and Y. Park, *Appl. Phys. Lett.* **80**, 3554 (2002).

<sup>5</sup>H. W. Jong and J. L. Lee, *J. Appl. Phys.* **93**, 5416 (2003).

<sup>6</sup>J. O. Song, D. S. Leem, J. S. Kwak, O. H. Nam, Y. Park, and T. Y. Seong, *Appl. Phys. Lett.* **83**, 2372 (2003).

<sup>7</sup>Y. J. Lin, Z. D. Li, C. W. Hsu, F. T. Chien, C. T. Lee, S. T. Shao, and H. C. Chang, *Appl. Phys. Lett.* **82**, 2817 (2003).

<sup>8</sup>J. S. Kwak, J. Cho, S. Chae, O. H. Nam, C. Sone, and Y. Park, *Jpn. J. Appl. Phys., Part 1* **40**, 6221 (2001).

<sup>9</sup>H. Kim, D. J. Kim, S. J. Park, and H. Hwang, *J. Appl. Phys.* **89**, 1506 (2001).

<sup>10</sup>D. Qiao, L. S. Yu, S. S. Lau, J. Y. Lin, H. X. Jiang, and T. E. Haynes, *J. Appl. Phys.* **88**, 4196 (2000).

<sup>11</sup>Y. Koide, T. Maeda, T. Kawakami, S. Fujita, T. Uemura, N. Shibata, and M. Murakami, *J. Electron. Mater.* **28**, 341 (1999).

<sup>12</sup>J. K. Sheu, Y. K. Su, G. C. Chi, P. L. Koh, M. J. Jou, C. M. Chang, C. C. Liu, and W. C. Hung, *Appl. Phys. Lett.* **74**, 2340 (1999).

<sup>13</sup>J. K. Ho, C. S. Jong, C. N. Huang, C. Y. Chen, C. C. Chiu, and K. K. Shih, *Appl. Phys. Lett.* **74**, 1275 (1999).

<sup>14</sup>J. K. Ho, C. S. Jong, C. N. Huang, C. C. Chiu, K. K. Shih, L. C. Chen, F. R. Chen, and J. J. Kai, *J. Appl. Phys.* **86**, 4491 (1999).

<sup>15</sup>S. H. Wang, S. E. Mohny, and R. Birkhahn, *J. Appl. Phys.* **91**, 3711 (2002).

<sup>16</sup>D. Mistele, F. Fedler, H. Klausling, T. Rotter, J. Stemmer, O. K. Semchinova, and J. Aderhold, *J. Cryst. Growth* **230**, 564 (2001).

<sup>17</sup>I. Waki, H. Fujioka, M. Oshima, H. Miki, and A. Fukizawa, *Appl. Phys. Lett.* **78**, 2899 (2001).

<sup>18</sup>K. A. Rickert, A. B. Ellis, J. K. Kim, J. L. Lee, F. J. Himpsel, F. Dwikusuma, and T. F. Kuech, *J. Appl. Phys.* **92**, 6671 (2002).

<sup>19</sup>L. S. Yu, D. Qiao, L. Jia, S. S. Lau, Y. Qi, and K. M. Lau, *Appl. Phys. Lett.* **79**, 4536 (2001).

<sup>20</sup>S. Nakamura, T. Mukai, M. Senoh, and N. Iwasa, *Jpn. J. Appl. Phys., Part 2* **31**, L139 (1992).

## Study of Schottky Barrier Heights of Indium-Tin-Oxide on p-GaN Using X-ray Photoelectron Spectroscopy and Current-Voltage Measurements

YOW-JON LIN<sup>1,2</sup> and CHOU-WEI HSU<sup>3</sup>

1.—Institute of Photonics, National Changhua University of Education, Changhua 500, Taiwan, Republic of China. 2—E-mail: rzt2390@yahoo.com.tw 3.—Department of Electrical Engineering, Feng Chia University, Taichung 407, Taiwan, Republic of China.

In this study, the current density-voltage (J-V) characteristic of Schottky diodes of indium-tin-oxide (ITO) contacts to p-type GaN (p-GaN) has been investigated. The calculated barrier-height value of ITO/p-GaN samples using the thermionic field-emission (TFE) model is 3.2 eV, which implies that the work function of ITO is equal to 4.3 eV. The result is supported by J-V measurements of ITO/n-type GaN Schottky diodes. On the other hand, the barrier height of ITO/p-GaN was also determined from x-ray photoelectron spectroscopy (XPS) data. The analysis of the XPS spectral shifts indicated that this observed barrier-height value of ITO/p-GaN by XPS is in good agreement with the value of 3.2 eV obtained from J-V measurements.

**Key words:** Gallium nitride (GaN), indium-tin-oxide (ITO), Schottky barrier height, thermionic field emission (TFE), x-ray photoelectron spectroscopy (XPS)

### INTRODUCTION

Recently, well-known transparent conducting films, such as indium-tin-oxide (ITO), have found wide use as electrodes for light-emitting diodes and Schottky photodiodes.<sup>1-4</sup> Both high-quality ITO ohmic<sup>4</sup> contacts to p-type GaN (p-GaN) and ITO Schottky<sup>5</sup> contacts to n-type GaN (n-GaN) were reported. However, to our knowledge, p-GaN Schottky diodes using ITO Schottky contacts were not reported before. Because the sum of barrier height of n and p types adds up to the bandgap 3.4 eV, the high barrier height is expected after the deposited metals on the p-GaN.<sup>5</sup> However, the contacts tend to exhibit very leaky Schottky characteristics.<sup>6,7</sup> In a previous report,<sup>8</sup> Yu et al. found the current transport with a tunnel component because of defect states located in the near-surface region of p-GaN. Therefore, the slope of  $\ln$  current-voltage (I-V) could not be analyzed using the thermionic emission (TE) model.<sup>8</sup> To our knowledge, observed barrier height of p-GaN Schottky diodes by I-V measurements was not reported before.

In this work, the applications of the thermionic field-emission (TFE) and field-emission (FE) models in the study of Schottky barrier heights of ITO on p-GaN from I-V measurements are reported. According to the result of fitting the parameters to the current density-voltage (J-V) characteristic in the TFE regime for ITO/p-GaN, the barrier-height value is about 3.2 eV. In addition, according to the Schottky theory, the work function of ITO was calculated to be 4.3 eV. This is supported by J-V measurements of ITO/n-GaN Schottky diodes.

### EXPERIMENTAL PROCEDURE

The epitaxial layers used in the experiments were grown on c-plane sapphire substrates using a metal-organic chemical-vapor deposition (MOCVD) system. Trimethylgallium (TMG), ammonia (NH<sub>3</sub>), and bis-cyclopentadienylmagnesium (CP<sub>2</sub>-Mg) were used as the Ga, N, and Mg sources, respectively. An undoped, GaN buffer layer with a thickness of 650 nm was grown on the sapphire substrate at 520°C, followed by the growth of a Mg-doped p-GaN layer (762 nm) at 1,100°C. The Mg concentration ([Mg]) was  $6 \times 10^{19} \text{ cm}^{-3}$  for all samples. The [Mg] in p-GaN was

(Received October 20, 2003; accepted May 28, 2004)



measured using secondary ion mass spectroscopy. The grown samples were annealed for the purpose of generating holes at 750°C for 30 min in an N<sub>2</sub> ambient. The samples were cleaned in chemical clean solutions of trichloroethylene, acetone, and methanol. Planar-type Schottky contacts were formed by electron-beam evaporation. Using the liftoff technique, Ni/Au (5 nm/5 nm) ohmic contacts were deposited and annealed at 500°C in air ambient for 10 min. The fabricated process of ohmic contacts with low specific contact resistance has been reported by Ho et al.<sup>9</sup> Good ohmic contacts help to obtain the actual Schottky characteristics from I-V measurements. Then, prior to depositing ITO (300 nm) on Schottky contacts with circular patterns, the samples were dipped into a 60°C (NH<sub>4</sub>)<sub>2</sub>S<sub>x</sub> solution for 30 min. The (NH<sub>4</sub>)<sub>2</sub>S<sub>x</sub> surface treatment will lead to obtaining the Schottky limit of the barrier height of metals/p-GaN. The Schottky dots were 200 μm in diameter; the surrounding ring of the ohmic contact was 400 μm in inner diameter and 600 μm in outer diameter. The ITO films were deposited by a radio-frequency (13.56 MHz) sputtering system. During the ITO deposition, argon and oxygen were used as the sputtering gases, and the substrate holder was not cooled. The diodes were characterized using I-V measurements with a Keithley Model-4200-SCS/F semiconductor parameter analyzer.

## EXPERIMENTAL RESULTS AND DISCUSSION

Figure 1 shows the J-V curve of ITO/p-GaN Schottky diodes under forward-bias condition at room

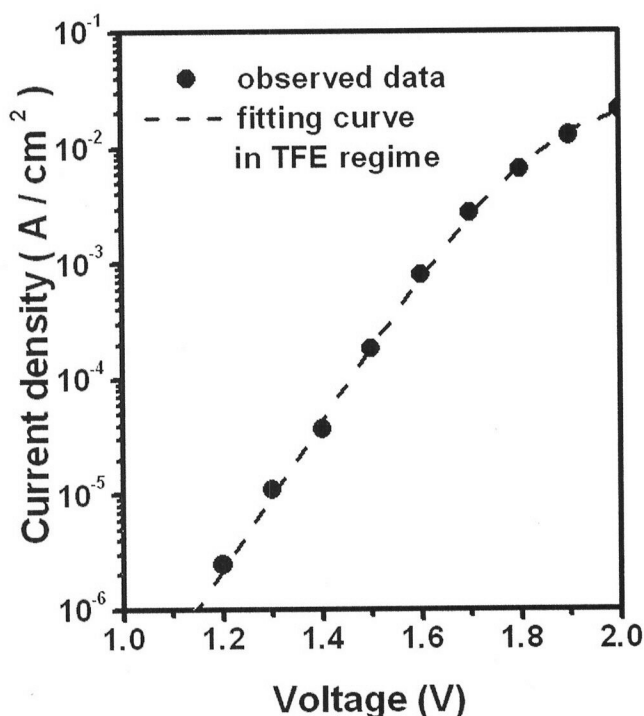


Fig. 1. The J-V curve of ITO/p-GaN Schottky diodes under forward-bias condition at RT and the fitting curve to the J-V characteristic in the TFE regime.

temperature (RT) and the fitting curve to the J-V characteristic in the TFE regime. These previous reports<sup>10,11</sup> provide theoretical analysis of tunneling current through a Schottky barrier ( $q\phi_B$ ). The J-V characteristic in the TFE regime can be described by the relation:<sup>10,11</sup>

$$J = J_S \exp [(qV - IR_s)/E_O - 1] \quad (1)$$

$$E_O = E_{OO} \coth (E_{OO}/kT) \quad (2)$$

$$J_O = \frac{A^* T [\pi E_{OO} q (\phi_B - V - \xi q)]^{0.5}}{k \cosh (E_{OO}/kT)} \exp \left[ -\frac{\xi}{kT} - \frac{q}{E_O} (\phi_B - \xi q) \right] \quad (3)$$

$$E_{OO} = (qh/4\pi) (N/m^* \epsilon)^{0.5} \quad (4)$$

where  $R_s$  is the series resistance,  $m^*$  ( $m^* = 0.6 m_o$ ,  $m_o$  is the mass of hole at rest)<sup>12</sup> is the hole effective mass,  $\epsilon$  ( $\epsilon = 9.5\epsilon_o$ ,  $\epsilon_o$  is the permittivity in vacuum)<sup>13</sup> is the dielectric constant of GaN,  $A^*$  ( $A^* = 103.8 \text{ A/cm}^2\text{K}^2$ )<sup>14</sup> is the effective Richardson constant of p-GaN,  $h$  is Planck's constant,  $V$  is the voltage,  $q$  is the electron charge,  $N$  is the doping concentration,<sup>8</sup> and  $\xi$  is the energy difference between the valence-band maximum ( $E_V$ ) and the Fermi level ( $E_F$ ). According to a previous report,<sup>15</sup> the  $E_F$  is located at 0.13 eV above the  $E_V$  of p-GaN with a hole concentration of  $2 \times 10^{17} \text{ cm}^{-3}$  at 300 K. In this study, a hole concentration of  $3.6 \times 10^{17} \text{ cm}^{-3}$  was obtained from Hall measurements. Therefore, the  $\xi$  was assumed to be equal to 0.1 eV in this study. The observed J-V curve of ITO/p-GaN Schottky diodes, as shown in Fig. 1, was fit using Eqs. 1–3. According to the fitting result (Fig. 1), the value of  $E_O$  and  $E_{OO}$  could be calculated to be 66 meV and 65 meV, respectively, and the value of  $R_s$  is about 25 kΩ. The large series resistance is attributed to the large spacing between Schottky and ohmic contact.<sup>5</sup> The deduced value of  $E_{OO}$  is likely to contain a tunneling component caused by defect states located in the near-surface region of the semiconductor in addition to the acceptor concentration ( $N$ ) expressed in Eq. 4.<sup>8</sup> The value of  $N$  was estimated to be  $7 \times 10^{19} \text{ cm}^{-3}$  using Eq. 4. The  $N$  of  $7 \times 10^{19} \text{ cm}^{-3}$  is similar to [Mg], which indicated that the tunneling current under forward-bias condition is attributed to the deep-level defect band induced by high Mg doping.<sup>16</sup> Kwak et al.<sup>16</sup> suggested that the current transport at the metal/heavy Mg-doped p-GaN interface was dominated by a deep-level defect band induced by high Mg doping. In addition, Yu et al.<sup>8</sup> indicated that the acceptor concentration was found to be  $10^{19} \text{ cm}^{-3}$  in the near-surface region of p-GaN when [Mg] in the doping layer was about  $10^{19}$ – $10^{20} \text{ cm}^{-3}$ . They found that the value was ~100 times higher than the hole concentration of  $\sim 10^{17} \text{ cm}^{-3}$  obtained from Hall measurements.<sup>8</sup> Our experimental result of the  $N$  (or [Mg]) of  $6$ – $7 \times 10^{19} \text{ cm}^{-3}$  yielding a hole concentration of  $3.6 \times 10^{17} \text{ cm}^{-3}$  is consistent with the reported values.<sup>17</sup> Besides, the  $q\phi_B$  of ITO/p-GaN samples was calculated to be 3.2 eV using Eq. 3. For the ITO/p-GaN Schottky diodes, the  $q\phi_B$  is also given by<sup>18</sup>



$$q\phi_B = \chi + E_g - W_{ITO} = 3.2 \text{ eV} \quad (5)$$

where  $W_{ITO}$  is the work function of ITO,  $\chi$  ( $\chi = 4.1 \text{ eV}$ )<sup>19</sup> is the electron affinity of GaN, and  $E_g$  ( $E_g = 3.4 \text{ eV}$ ) represents the bandgap of GaN at RT. The work function of ITO was calculated to be 4.3 eV using Eq. 5. The estimated work-function value of ITO is similar to the values reported by Milliron et al.<sup>20</sup> and Nüesch et al.<sup>21</sup>

On the other hand, the J-V characteristics in the FE regime are given by<sup>10</sup>

$$J = J_f \exp [(qV)/E_{OO}] \quad (6)$$

$$J_f = \frac{\pi A * T}{k C_1 \sin(\pi k T C_1)} \exp\left(-\frac{q\phi_B}{E_{OO}}\right) \quad (7)$$

$$C_1 = (2E_{OO})^{-1} \ln[-4q(\phi_B - V)/\xi] \quad (8)$$

The observed current is too small to obtain the fitting parameters to the J-V characteristic in the FE regime for ITO/p-GaN. This suggests that the FE model cannot be used to study the  $q\phi_B$  in this case. In addition, the  $E_{OO}$  of 65 meV is not much greater than  $kT$ , so the FE will not happen.<sup>10</sup> To our knowledge, the effective resistance of the Schottky barrier in the FE regime is quite low, so the FE model is often used for ohmic contact.<sup>10</sup>

To further confirm whether the barrier-height calculation and the work-function calculation in the TFE regime are correct, the ITO/n-GaN Schottky diodes have to be fabricated, and the J-V characteristics of ITO/n-GaN Schottky diodes must be understood. The epitaxial layers of n-GaN samples used in this work were grown on c-plane sapphire (0001) by the MOCVD technique. An undoped GaN layer with a thickness of 650 nm was grown on the sapphire substrate at 520°C, followed by a 1.2- $\mu\text{m}$ -thick n-GaN layer doped with Si at 1,050°C. For the n-GaN layer, the carrier concentration and mobility were  $6.2 \times 10^{17} \text{ cm}^{-3}$  and  $245 \text{ cm}^2/\text{V}\cdot\text{s}$ , respectively. Ohmic contacts consisting of a rapid thermally annealed Ti/Al (50 nm/150 nm) bilayer were first prepared on the n-GaN epilayer. Then, prior to the deposited ITO (300 nm) on Schottky contacts with circular patterns, the samples were dipped into the 60°C  $(\text{NH}_4)_2\text{S}_x$  solution for 20 min. The pattern of ITO/n-GaN Schottky diodes is the same as the pattern of ITO/p-GaN Schottky diodes, as discussed previously. A linear behavior was found from J-V measurements of ITO/ n-GaN Schottky diodes, as shown in Fig. 2. The ITO has a work function of 4.3 eV, which was obtained from the Schottky theory and J-V measurements of ITO/p-GaN. This value (4.3 eV) is near the electron affinity of n-GaN. If they are in intimate contact, a low energy barrier between ITO and n-GaN will lead to ohmic contact formation. This implies that the TFE model can be used to calculate the barrier height of ITO/p-GaN Schottky diodes. On the other hand, Schmitz et al.<sup>22</sup> have indicated that the linear nature of the I-V characteristics for the Schottky diodes of Al/n-GaN suggested its potential use in forming ohmic con-

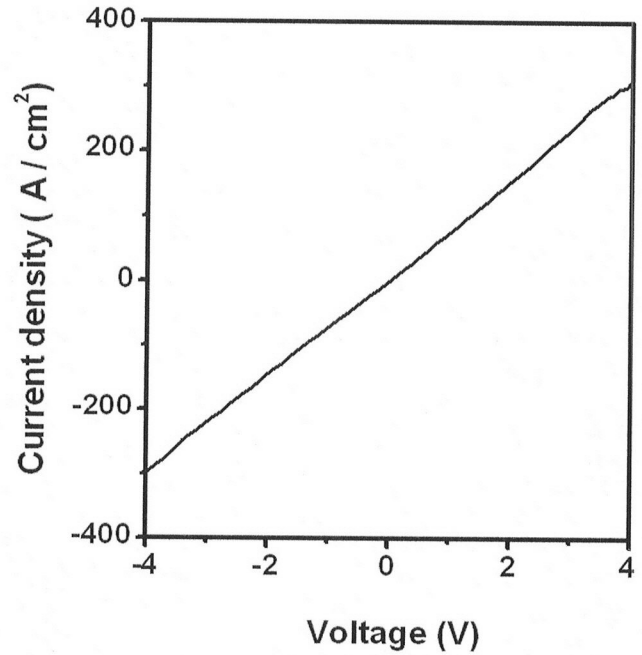


Fig. 2. The J-V curve of ITO/n-GaN Schottky diodes at RT.

tacts. The Al has a work function of 4.28 eV.<sup>22</sup> This value of 4.28 eV is near the estimated value of the work function of ITO in this work. On the basis of the evidence, we deduce that the estimated work-function value (4.3 eV) of ITO and barrier-height value (3.2 eV) of ITO/p-GaN Schottky diodes are reliable. Besides, this also suggested that n-GaN devices using ITO ohmic contacts could be achieved, which will be further investigated in the future.

To further confirm whether the barrier-height value of ITO/p-GaN Schottky diodes is 3.2 eV, x-ray photoelectron spectroscopy (XPS) is used to study the surface Fermi-level position within the bandgap for the ITO overlayer on p-GaN. The XPS measurements were performed using a monochromatic Al  $K_{\alpha}$  x-ray source. We took an Au  $4f_{7/2}$  peak at 83.86 eV and a Cu  $2p_{3/2}$  peak at 932.65 eV for energy reference purposes. The XPS analysis can be combined with argon ion-sputter etching to obtain a depth profile of the interfacial layer. The barrier height was determined from the XPS data using the relation shown in Eq. 9.<sup>23,24</sup> This equation was previously employed by Tracy et al.<sup>25</sup> for the calculation of the barrier heights ( $q\phi_n$ ) of metals on n-GaN.

$$q\phi_n = E_G - E_V^i + (E_{\text{core}}^i - E_{\text{core}}^m) = E_G - (E_{\text{core}}^m - E_{\text{VC}}) \quad (9)$$

where  $E_G$  is the bandgap of the semiconductor,  $E_{\text{core}}^m$  is the binding energy of the semiconductor core-level peak following metal deposition,  $E_{\text{core}}^i$  is the initial binding energy of the core-level peak,  $E_V^i$  is the initial binding energy of the  $E_V$  of the semiconductor, and  $E_{\text{VC}}$  is equal to  $(E_{\text{core}}^i - E_V^i)$ . All binding energies are measured relative to  $E_F$ . For the calculation of the barrier heights ( $q\phi_p$ ) of ITO/p-GaN, the equation is expressed as

$$q\phi_p = E_{\text{core}}^{\text{ITO}} - E_{\text{VC}} \quad (10)$$

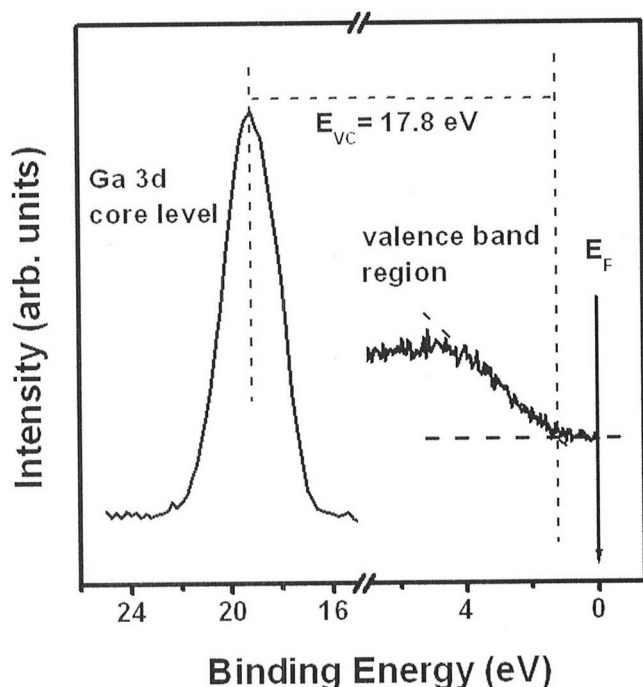


Fig. 3. The left spectrum shows the Ga 3d core-level peak on p-GaN without an ITO overlayer. The right figure presents the spectrum of the valence-band region. A linear fit is used to determine the energy of the valence-band edge.

where  $E_{\text{ITO}}^{\text{ITO}}$  is the binding energy of the p-GaN core-level peak following ITO deposition.

Figure 3 shows an example of the Ga 3d core level and the valence-band spectrum collected on the p-GaN sample without an ITO overlayer. The  $E_{\text{VC}}$  is calculated to be 17.8 eV. This value is in good agreement with the value of 17.8 eV reported by Hashizume et al.,<sup>26</sup> Bermudez,<sup>27</sup> Waldrop and Grant,<sup>28</sup> and Wu and Kahn.<sup>29</sup> Figure 4 shows the Ga 3d core level at the ITO/p-GaN interface after removal of the O 2s spectrum. The spectra determine the Ga 3d binding-energy  $E_{\text{ITO}}^{\text{ITO}}$  relative to  $E_{\text{F}}$ . In Fig. 4, we can see that  $E_{\text{ITO}}^{\text{ITO}}$  is equal to 20.9 eV. Therefore, the  $q\phi_{\text{p}}$  was calculated to be 3.1 eV, according to Eq. 10. This value is similar to the value of 3.2 eV obtained from J-V measurements.

### CONCLUSIONS

In summary, the J-V characteristics of Schottky diodes of ITO contacts to p-GaN and n-GaN have been investigated in this study. For the ITO/p-GaN Schottky diode, the barrier-height value calculated in the TFE regime is 3.2 eV. It can be derived that the work function of ITO may be equal to 4.3 eV. According to the observed results by J-V and XPS measurements, we deduce that the TFE model can be used to study the Schottky barrier height of ITO/p-GaN Schottky diodes.

### ACKNOWLEDGEMENTS

The authors thank Hsiang-Ping Wen and the National Science Council of the Republic of China for their support of this work (Grant Nos. NSC 91-2218-

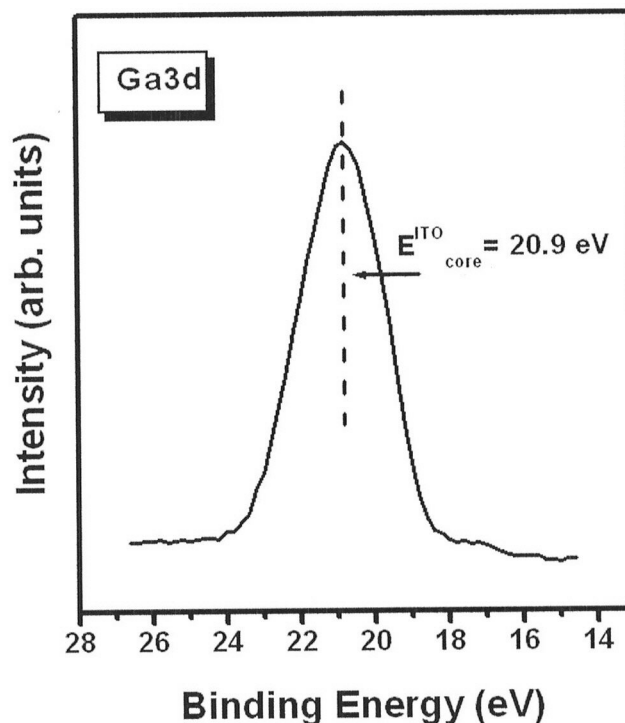


Fig. 4. The Ga 3d core level at the ITO/p-GaN interface. The binding energy is referenced to the Fermi level.

E-035-007 and NSC 93-2215-E-018-005). The x-ray photoelectron spectroscopy was kindly provided from the NTU Instrumentation Center at Taipei National Taiwan University.

### REFERENCES

1. S.Y. Kim, H.W. Jang, and J.L. Lee, *Appl. Phys. Lett.* 82, 61 (2003).
2. R.H. Horng, D.S. Wu, Y.C. Lien, and W.H. Lan, *Appl. Phys. Lett.* 79, 2925 (2001).
3. N. Biyikli, T. Kartaloglu, O. Aytur, I. Kimukin, and E. Ozbay, *Appl. Phys. Lett.* 79, 2838 (2001).
4. T. Margalith, O. Buchinsky, D.A. Cohen, A.C. Abare, M. Hansen, S.P. DenBaars, and L.A. Coldren, *Appl. Phys. Lett.* 74, 3930 (1999).
5. J.K. Shen, Y.K. Su, G.C. Chi, M.J. Jou, and C.M. Chang, *Appl. Phys. Lett.* 72, 3317 (1998).
6. T. Mori, T. Kozawa, T. Ohwaki, Y. Taga, S. Naagai, S. Yamasaki, S. Asami, N. Shibata, and M. Koike, *Appl. Phys. Lett.* 69, 3537 (1996).
7. H. Ishikawa, S. Kobayashi, Y. Koide, S. Yamasaki, S. Nagai, J. Umezaki, M. Koike, and M. Murakami, *J. Appl. Phys.* 81, 1315 (1997).
8. L.S. Yu, D. Qiao, L. Jia, S.S. Lau, Y. Qi, and K.M. Lau, *Appl. Phys. Lett.* 79, 4536 (2001).
9. J.K. Ho, C.S. Jong, C.N. Huang, C.C. Chiu, K.K. Shih, L.C. Chen, F.R. Chen, and J.J. Kai, *J. Appl. Phys.* 86, 4491 (1999).
10. M. Shur, *Physics of Semiconductor Devices* (Englewood Cliffs, NJ: Prentice-Hall, 1990), pp. 204–209.
11. H. Morkoç, *Nitride Semiconductors and Devices* (Berlin: Springer, 1999), pp. 198–200.
12. C. Merz, M. Kunzer, U. Kaufmann, I. Akasaki, and H. Amano, *Semicond. Sci. Technol.* 11, 712 (1996).
13. M. Razeghi and A. Rogalski, *J. Appl. Phys.* 79, 7433 (1996).
14. J.I. Pankove, S. Bloom, and G. Harbecke, *RCA Rev.* 36, 163 (1975).
15. H. Nakayama, P. Hacke, M.R.H. Khan, T. Detch-Prohm, K. Hiramatsu, and N. Sawaki, *Jpn. J. Appl. Phys.* 35, L282 (1996).

16. J.S. Kwak, O.H. Nam, and Y. Park, *Appl. Phys. Lett.* 80, 3554 (2002).
17. P. Kozodoy, H. Xing, S.P. DenBaars, U.K. Mishra, A. Saxler, R. Perrin, S. Elhamri, and W.C. Mitchel, *J. Appl. Phys.* 87, 1832 (2000).
18. B.L. Sharma, *Metal-Semiconductor Schottky Barrier Junctions and Their Applications* (New York: Plenum Press, 1984), pp. 2-8.
19. S. Arulkumaran, T. Egawa, H. Ishikawa, T. Jimbo, and M. Umeno, *Appl. Phys. Lett.* 73, 809 (1998).
20. D.J. Milliron, I.G. Hill, C. Shen, A. Kahn, and J. Schwartz, *J. Appl. Phys.* 87, 572 (2000).
21. F. Nüesch, L.J. Rothberg, E.W. Forsythe, Q.T. Le, and Y. Gao, *Appl. Phys. Lett.* 74, 880 (1999).
22. A.C. Schmitz, A.T. Ping, M.A. Khan, Q. Chen, J.W. Yang, and I. Adesida, *J. Electron. Mater.* 27, 255 (1998).
23. J.R. Waldrop and R.W. Grant, *Appl. Phys. Lett.* 52, 1794 (1988).
24. J.R. Waldrop and R.W. Grant, *Appl. Phys. Lett.* 62, 2685 (1993).
25. K.M. Tracy, P.J. Hartlieb, S. Einfeldt, F. Davis, E.H. Hurt, and R.J. Nemanich, *J. Appl. Phys.* 94, 3939 (2003).
26. T. Hashizume, S. Ootomo, S. Oyama, M. Konishi, and H. Hasegawa, *J. Vac. Sci. Technol. B* 19, 1675 (2001).
27. V.M. Bermudez, *J. Appl. Phys.* 80, 1190 (1996).
28. J.R. Waldrop and R.W. Grant, *Appl. Phys. Lett.* 68, 2879 (1996).
29. C.I. Wu and A. Kahn, *J. Appl. Phys.* 86, 3209 (1999).